THE COMPLEX BINARY FOURIER REPRESENTATION

by

TEJKARAN R. AGRAWAL

B. E. (Elect. Engg.), 1968
Shri G. S. Technological Institute,
University of Indore, Indore (M. P.)
INDIA

A MASTER'S REPORT

submitted in partial fulfillment of the

requirements for the degree

MASTER OF SCIENCE

Department of Electrical Engineering

KANSAS STATE UNIVERSITY
Manhattan, Kansas

1970

Approved by:

Nasir Ahmed

Major Professor

TABLE OF CONTENTS

LIST OF FIGURES

CHAPTER I

INTRODUCTION

Given a sequence $x(j)$, $j = 0, 1, 2, \ldots, (N-1)$, obtained by sampling a continuous waveform, one seeks its frequency structure by means of an orthogonal transformation which maps the $x(j)$ into a sequence $A(n)$, $n = 0, 1, 2, \ldots, (N-1)$. If $F_n(j)$ are a set of N orthonormal functions, it follows that

$$A(n) = \sum_{j=0}^{N-1} x(j) \quad F_n(j), \; n = 0, 1, 2, \ldots, (N-1) . \qquad (1.1)$$

Most of the work in this area has been done for the case when the set $F_n(j)$ are the Fourier functions. The corresponding transform is the so-called discrete Fourier transform (DFT). Again, the Fast Fourier transform (FFT) is an algorithm which yields the desired coefficients $A(n)$ in approximately $2N \cdot \log_2 N$ arithmetic operations and affords a substantial saving in memory [1]. A less publicized transform is the BIFORE (Binary Fourier Representation) transform* (BT) [2, 3] in which the bases are square waves (Walsh functions). Periodic sampling of these square waves yields Hadamard matrices [4] which possess transform properties. The corresponding algorithm which requires $N \cdot \log_2 N$ arithmetic operations to obtain the $A(n)$ in (1.1) is called the Fast BIFORE or Hadamard transform (FBT) [2]. A BIFORE power spectrum which possesses the shift invariance property similar to the conventional Fourier spectrum has been developed [3]. The BT has found applications in several areas which include signal representation and classification [2], image coding [5], spectral analysis of linear digital systems [6] and speech processing [7, 8] . Several of its properties have

---

*Also called the Hadamard or Walsh-Fourier transform.

been developed and compared with corresponding properties of the DFT [9, 10] .

This report concerns a study of a more general version of the BT, namely the complex BIFORE transform (CBT) [11] .

In Chapter II, the notion of complex Binary Fourier Representation is introduced. Chapter III presents a development of the CBT power spectrum. In Chapter IV, a physical interpretation of the CBT power spectrum is presented. Finally, recommendations for future work are included in Chapter V.

Since the CBT is a more general version of the BT, it is reasonable to expect that it will find applications in several areas in addition to those cited above with respect to the BT.

CHAPTER II

COMPLEX BINARY FOURIER REPRESENTATION

2.1 Complex Hadamard Matrices

Walsh functions [3] are a set of orthogonal functions which are square waves. Consequently, the amplitude of a Walsh function is either +1 or -1. Sampling of Walsh functions results in an array whose elements are ±1. A rearrangement of the rows of such an array yields real Hadamard matrices which can be defined by the following recursion formula:

$$\left[H(k)\right] = \left[\begin{array}{c|c} H(k-1) & H(k-1) \\ \hline H(k-1) & -H(k-1) \end{array}\right], \quad k = 1, 2, \ldots, n \tag{2.1}$$

where $\left[H(k)\right]$ is a $(2^k \times 2^k)$ Hadamard matrix, $\left[H(0)\right] = \left[1\right]$

and $n = \log_2 N$.

Again, the complex version of the Hadamard matrices in (2.1) are defined by the recursion formula

$$\left[H_c(k)\right] = \left[\begin{array}{c|c} H_c(k-1) & H_c(k-1) \\ \hline P(1) \otimes H(k-2) & -P(1) \otimes H(k-2) \end{array}\right] \tag{2.2}$$

for $k = 1, 2, \ldots, n$,

where $\left[H_c(k)\right]$ is a $(2^k \times 2^k)$ complex Hadamard matrix,

$\left[H_c(0)\right] = \left[1\right]$,

$\otimes$ implies the Kronecker delta product (see Appendix A) and

$$\left[P(1)\right] = \begin{bmatrix} 1 & -i \\ 1 & i \end{bmatrix}, \quad i = \sqrt{-1} \ .$$

For example, for $k = 1$ and $k = 2$, (2.2) yields

$$\left[H_c(1)\right] = \begin{bmatrix} 1 & 1 \\ 1 & -1 \end{bmatrix}$$

and

$$\left[H_c(2)\right] = \begin{bmatrix} 1 & 1 & 1 & 1 \\ 1 & -1 & 1 & -1 \\ 1 & -i & -1 & i \\ 1 & i & -1 & -i \end{bmatrix}$$

respectively.

From. (2.2) and the definition of Kronecker delta product it follows that

$$\left[H_c(k)\right] = \left[\begin{array}{c|c} H_c(k-1) & H_c(k-1) \\ \hline H(k-2) & -iH(k-2) \\ \hline H(k-2) & iH(k-2) \end{array} \begin{array}{c|c} & \\ \hline -H(k-2) & iH(k-2) \\ \hline -H(k-2) & -iH(k-2) \end{array}\right] \qquad (2.3)$$

for $k = 1, 2, \ldots, n$,

where, $\left[H_c(0)\right] = \left[1\right]$.

For example with k = 3, Eq. (2.3) yields

$$\left[H_c(3)\right] = \left[\begin{array}{cccc|cccc} 1 & 1 & 1 & 1 & 1 & 1 & 1 & 1 \\ 1 & -1 & 1 & -1 & 1 & -1 & 1 & -1 \\ 1 & -i & -1 & i & 1 & -i & -1 & i \\ 1 & i & -1 & -i & 1 & i & -1 & -i \\ \hline 1 & 1 & -i & -i & -1 & -1 & i & i \\ 1 & -1 & -i & i & -1 & 1 & i & -i \\ 1 & 1 & i & i & -1 & -1 & -i & -i \\ 1 & -1 & i & -i & -1 & 1 & -i & i \end{array}\right]$$

2.2 Orthogonal Properties of Complex Hadamard Matrices

The complex Hadamard matrix satisfy the orthogonal property

$$\left[H_c(n)\right] \left[H_c^*(n)\right]^T = N\left[I(n)\right] \qquad (2.4)$$

where, $N = 2^n$,

$\left[H_c^*(n)\right]^T$ is the transpose of complex conjugate of $\left[H_c(n)\right]$,

$\left[I(n)\right]$ is the identity matrix of order 2^n. For example, for n = 2,

(2.4) yields

$$\begin{bmatrix} 1 & 1 & 1 & 1 \\ 1 & -1 & 1 & -1 \\ 1 & -i & -1 & i \\ 1 & i & -1 & -i \end{bmatrix} \begin{bmatrix} 1 & 1 & 1 & 1 \\ 1 & -1 & i & -i \\ 1 & 1 & -1 & -1 \\ 1 & -1 & -i & i \end{bmatrix} = \begin{bmatrix} 4 & 0 & 0 & 0 \\ 0 & 4 & 0 & 0 \\ 0 & 0 & 4 & 0 \\ 0 & 0 & 0 & 4 \end{bmatrix}$$

or $$\left[H_c(2)\right] \left[H_c^*(2)\right]^T = 4\left[I(2)\right] .$$

Since $\left[H_c(n)\right]$ is orthogonal, its inverse can be found as follows

$$\left[H_c(n)\right] \left[H_c(n)\right]^{-1} = \left[I(n)\right] . \tag{2.5}$$

Comparison of (2.4) and (2.5) results in

$$\left[H_c(n)\right]^{-1} = \frac{1}{N} \left[H_c^*(n)\right]^T . \tag{2.6}$$

2.3 Complex BIFORE Transform (CBT)

Denoting the sequence x(j), j = 0, 1, . . ., (N-1) by $\left[X(n)\right]$, the complex BIFORE (Binary Fourier Representation) transform is defined as

$$\left[B_x(n)\right] = \frac{1}{N} \left[H_c(n)\right] \left[X(n)\right] \tag{2.7}$$

where

$\left[X(n)\right]^T = \left[x(0) \quad x(1) \quad x(2) \ldots\ldots x(N-1)\right]$ is the vector representation of the data sequence $\left[X(n)\right]$,

$\left[B_x(n)\right]^T = \left[B(0) \quad B(1) \quad B(2) \ldots\ldots B(N-1)\right]$, the B(k) being the transformed coefficients and $\left[H_c(n)\right]$ is the (NxN) complex Hadamard matrix defined in (2.3).

2.4 Fast Complex BIFORE Transform (FCBT)

The FCBT is an algorithm which facilitates rapid computation of the transform coefficients B(k), k = 0, 1, . . ., (N-1). The development of the algorithm is best illustrated for N = 8, when (2.7) yields

$$\left[B_x(3)\right] = \frac{1}{8} \left[H_c(3)\right] \left[X(3)\right] ;$$

that is

$$\begin{bmatrix} B(0) \\ B(1) \\ B(2) \\ B(3) \\ B(4) \\ B(5) \\ B(6) \\ B(7) \end{bmatrix} = \frac{1}{8} \left[\begin{array}{cc|cc} \multicolumn{2}{c|}{H_c(2)} & \multicolumn{2}{c}{H_c(2)} \\ \hline H(1) & -iH(1) & -H(1) & iH(1) \\ H(1) & iH(1) & -H(1) & -iH(1) \end{array}\right] \begin{bmatrix} x(0) \\ x(1) \\ x(2) \\ x(3) \\ x(4) \\ x(5) \\ x(6) \\ x(7) \end{bmatrix} . \quad (2.8)$$

Solving for first four points, one has

$$\begin{bmatrix} B(0) \\ B(1) \\ B(2) \\ B(3) \end{bmatrix} = \frac{1}{8} \begin{bmatrix} H_c(2) \end{bmatrix} \begin{bmatrix} x(0) + x(4) \\ x(1) + x(5) \\ x(2) + x(6) \\ x(3) + x(7) \end{bmatrix} .$$

Decomposing $\begin{bmatrix} H_c(2) \end{bmatrix}$ into lower order Hadamard matrices and recalling that $\begin{bmatrix} H_c(1) \end{bmatrix} = \begin{bmatrix} H(1) \end{bmatrix}$,

the above expression yields

$$\begin{bmatrix} B(0) \\ B(1) \\ B(2) \\ B(3) \end{bmatrix} = \frac{1}{8} \left[\begin{array}{cc|cc} \multicolumn{2}{c|}{H(1)} & \multicolumn{2}{c}{H(1)} \\ \hline H(0) & -iH(0) & -H(0) & iH(0) \\ H(0) & iH(0) & -H(0) & -iH(0) \end{array}\right] \begin{bmatrix} x(0) + x(4) \\ x(1) + x(5) \\ x(2) + x(6) \\ x(3) + x(7) \end{bmatrix} . \quad (2.9)$$

The last four points in (2.8) give an expression

$$\begin{bmatrix} B(4) \\ B(5) \\ B(6) \\ B(7) \end{bmatrix} = \frac{1}{8} \left[\begin{array}{c|c} H(1) & -iH(1) \\ \hline H(1) & iH(1) \end{array}\right] \begin{bmatrix} x(0) - x(4) \\ x(1) - x(5) \\ x(2) - x(6) \\ x(3) - x(7) \end{bmatrix} . \quad (2.10)$$

The additions and subtractions associated with (2.9) and (2.10) are designated by Iteration 1 in the signal flow graph for N = 8 shown in Fig.(2.1) where

$$x_1(k) = x(k) + x(k+4),\ k = 0, 1, 2, 3$$

and

$$x_1(k) = x(k-4) - x(k),\ k = 4, 5, 6, 7 \ . \tag{2.11}$$

The notations used for signal flow graphs throughout the work are explained below

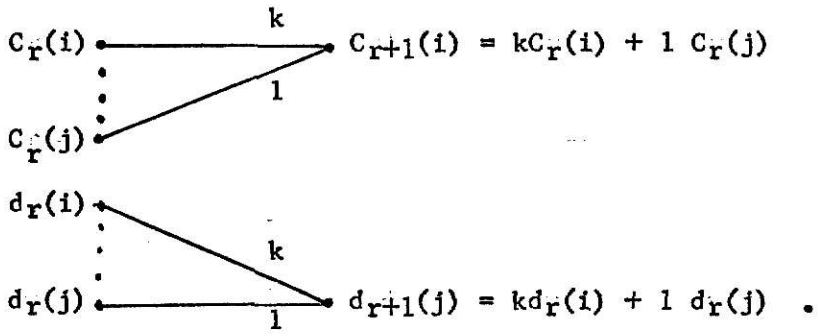

This represents the $(r+1)^{th}$ iteration. The multiplier is 1 if nothing is mentioned.

Substituting (2.11) into (2.9) there results

$$\begin{bmatrix} B(0) \\ B(1) \\ B(2) \\ B(3) \end{bmatrix} = \frac{1}{8} \left[\begin{array}{c|c|c|c} & H(1) & & H(1) \\ \hline H(0) & -iH(0) & -H(0) & iH(0) \\ \hline H(0) & iH(0) & -H(0) & -iH(0) \end{array}\right] \begin{bmatrix} x_1(0) \\ x_1(1) \\ x_1(2) \\ x_1(3) \end{bmatrix} \ . \tag{2.12}$$

Again from (2.12) one has

$$\begin{bmatrix} B(0) \\ B(1) \end{bmatrix} = \frac{1}{8} \begin{bmatrix} H(1) \end{bmatrix} \begin{bmatrix} x_1(0) + x_1(2) \\ x_1(1) + x_1(3) \end{bmatrix}$$

or

$$= \frac{1}{8} \begin{bmatrix} 1 & 1 \\ 1 & -1 \end{bmatrix} \begin{bmatrix} x_2(0) \\ x_2(1) \end{bmatrix} \tag{2.13}$$

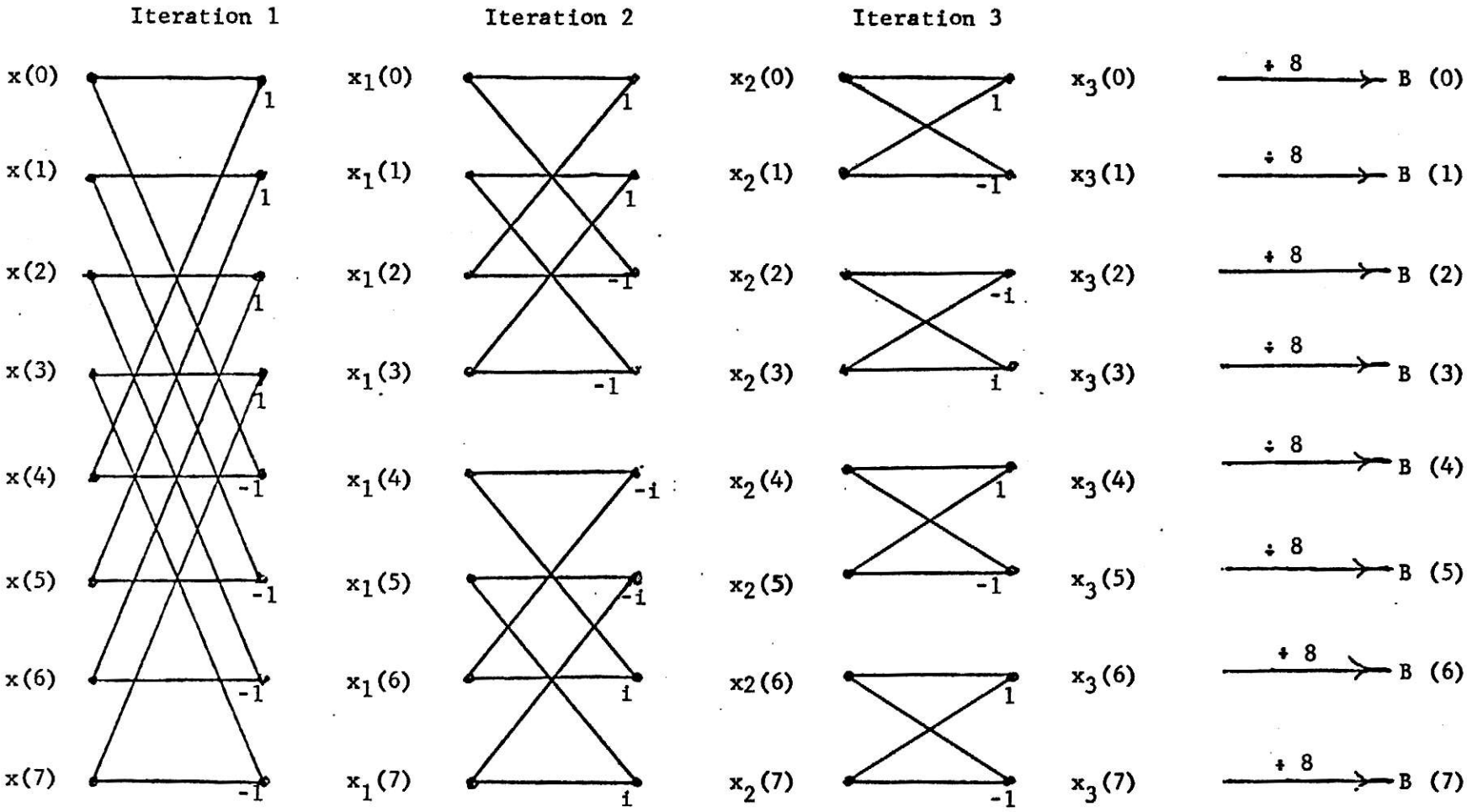

Fig. (2.1). Signal flow graph of FCBT for N = 8.

where $x_2(0) = x_1(0) + x_1(2)$

$x_2(1) = x_1(1) + x_1(3)$.

The additions and subtractions in (2.13) are represented by iteration 2 in Fig.(2.1).

Evaluation of (2.13) yields

$$B(0) = \frac{1}{8} x_3(0)$$

and (2.14)

$$B(1) = \frac{1}{8} x_3(1)$$

where $x_3(0) = x_2(0) + x_2(1)$

and $x_3(1) = x_2(0) - x_2(1)$.

Iteration 3 in Fig.(2.1) shows the arithmetic operations in (2.14).

Again from (2.12) and (2.14) it follows that

$$\begin{bmatrix} B(2) \\ B(3) \end{bmatrix} = \frac{1}{8} \begin{bmatrix} H(0) & -iH(0) \\ H(0) & iH(0) \end{bmatrix} \begin{bmatrix} x_2(2) \\ x_2(3) \end{bmatrix} . \tag{2.15}$$

The additions and subtractions which lead to (2.15) are shown in Fig.(2.1) and designated by iteration 2. On simplification, (2.15) yields

$$B(2) = \frac{1}{8} x_3(2)$$

and $B(3) = \frac{1}{8} x_3(3)$

where $x_3(2) = x_2(2) - i\, x_2(3)$

and $x_3(3) = x_2(2) + i\, x_2(3)$.

Now going back to (2.10), one has

$$\begin{bmatrix} B(4) \\ B(5) \\ B(6) \\ B(7) \end{bmatrix} = \frac{1}{8} \begin{bmatrix} H(1) & -iH(1) \\ H(1) & iH(1) \end{bmatrix} \begin{bmatrix} x_1(4) \\ x_1(5) \\ x_1(6) \\ x_1(7) \end{bmatrix} . \tag{2.16}$$

Matrix partitioning of (2.16) yields

$$\begin{bmatrix} B(4) \\ B(5) \end{bmatrix} = \frac{1}{8} \begin{bmatrix} 1 & 1 \\ 1 & -1 \end{bmatrix} \begin{bmatrix} x_2(4) \\ x_2(5) \end{bmatrix} \tag{2.17}$$

where

$$\begin{bmatrix} x_2(4) \\ x_2(5) \end{bmatrix} = \begin{bmatrix} x_1(4) - i\, x_1(6) \\ x_1(4) + i\, x_1(6) \end{bmatrix} .$$

Figure (2.1) shows the arithmetic operations in (2.17) under iteration 2.

Then (2.16) on simplification yields

$$B(4) = \frac{1}{8} x_3(4) \tag{2.18}$$

and

$$B(5) = \frac{1}{8} x_3(5)$$

where

$$x_3(4) = x_2(4) + x_2(5)$$

and

$$x_3(5) = x_2(4) - x_2(5) .$$

Iteration 3 in Fig. (2.1) shows the arithmetic operations in (2.18).

Finally, from the lower half of (2.16), it follows that

$$\begin{bmatrix} B(6) \\ B(7) \end{bmatrix} = \frac{1}{8} \begin{bmatrix} 1 & 1 \\ 1 & -1 \end{bmatrix} \begin{bmatrix} x_2(6) \\ x_2(7) \end{bmatrix} \tag{2.19}$$

where

$$x_2(6) = x_1(4) + i\, x_1(6)$$

and

$$x_2(7) = x_1(5) + i\, x_1(7) \; ;$$

that is

$$B(6) = \frac{1}{8} x_3(6) \tag{2.20}$$

and

$$B(7) = \frac{1}{8} x_3(7)$$

where

$$x_3(6) = x_2(6) + x_2(7)$$

and

$$x_3(7) = x_2(6) - x_2(7) .$$

The arithmetic operations in (2.18) and (2.19) are shown under iteration 2 and iteration 3 respectively in Fig. (2.1).

This concludes the development of the algorithm for computing the BIFORE transform for complex input sequences. As a further illustration, the signal flow graph for N = 16 is also included in Fig. (2.2).

Generalizations

Examination of the signal flow graphs in Figs. (2.1) and (2.2), leads to the following observations and subsequent generalization.

1. There are $\log_2 N$ iterations for a N-periodic sequence.

2. The first iteration consists of additions and subtractions only since the multipliers are ± 1.

3. After the first iteration, $\frac{N}{2}$ data points in the lower half take multipliers -i and i. The multiplier -i is associated with the $\frac{N}{4}$ data points in the upper half portion, while the lower half portion takes the multiplier i.

4. The $\frac{N}{2}$ points in the lower half, then, follow ordinary BIFORE transform with real multipliers ± 1 for the remaining $\left(\log_2 N - 2\right)$ iterations.

5. After the 1st iteration the upper half of $\frac{N}{2}$ points is treated as a new set of $\frac{N}{2}$ points and CBT is performed over them from step 2 explained above.

To illustrate the CBT for N = 8 and N = 16, examples are considered in Fig. 2.3 and Fig. 2.4.

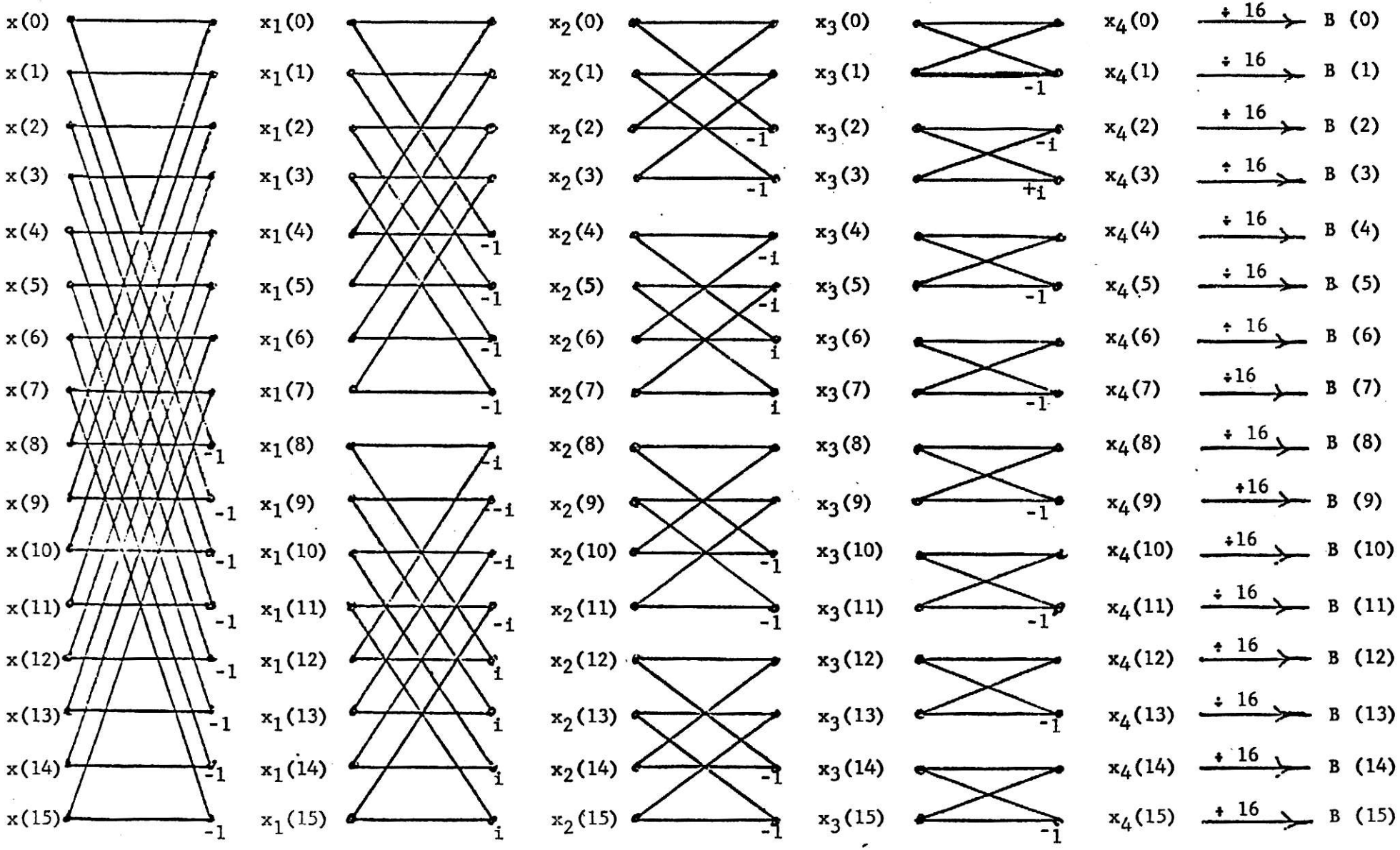

Fig. (2.2). FCBT signal flow graph for N = 16.

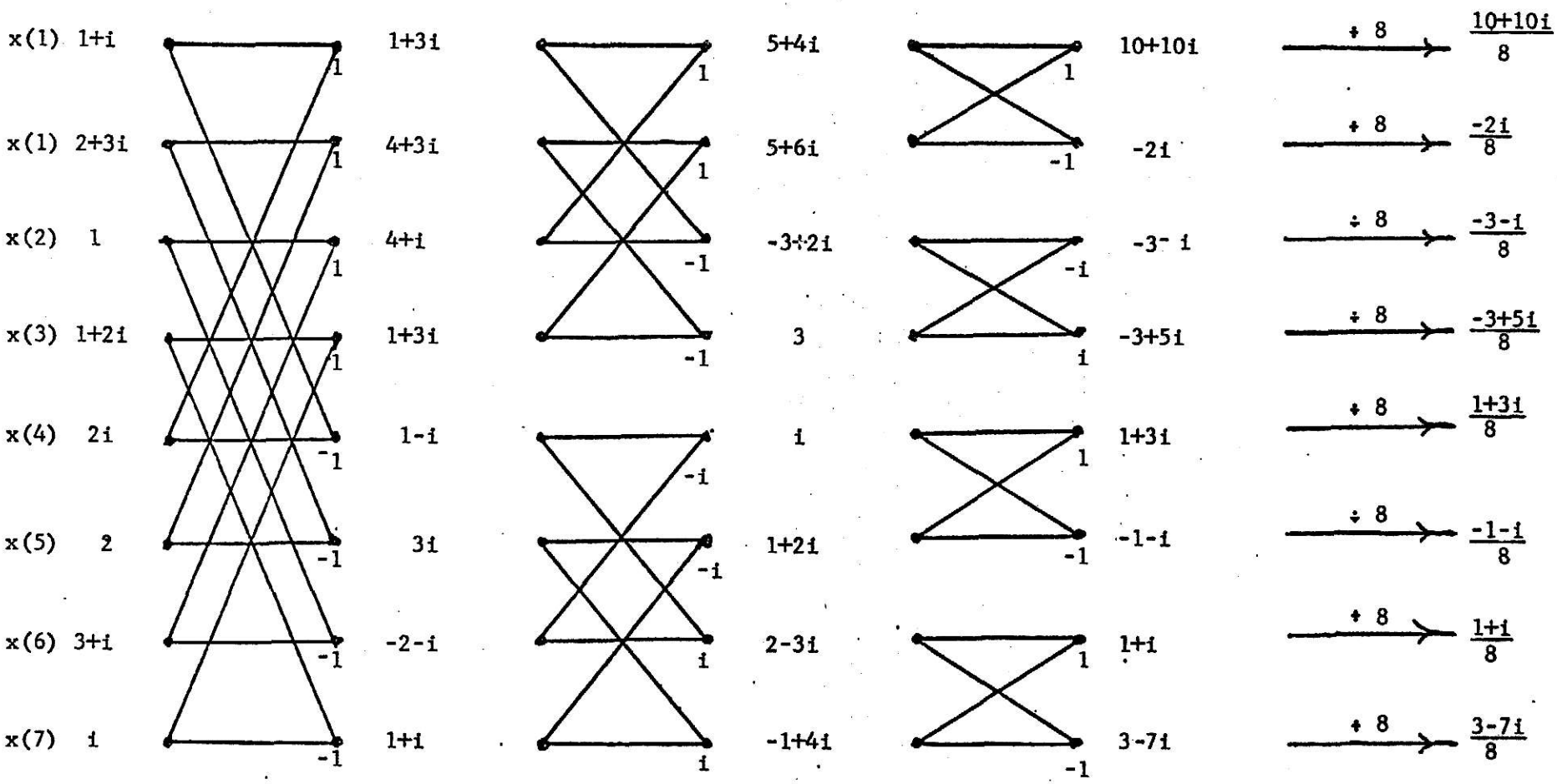

Fig. (2.3). Example of CBT for N = 8.

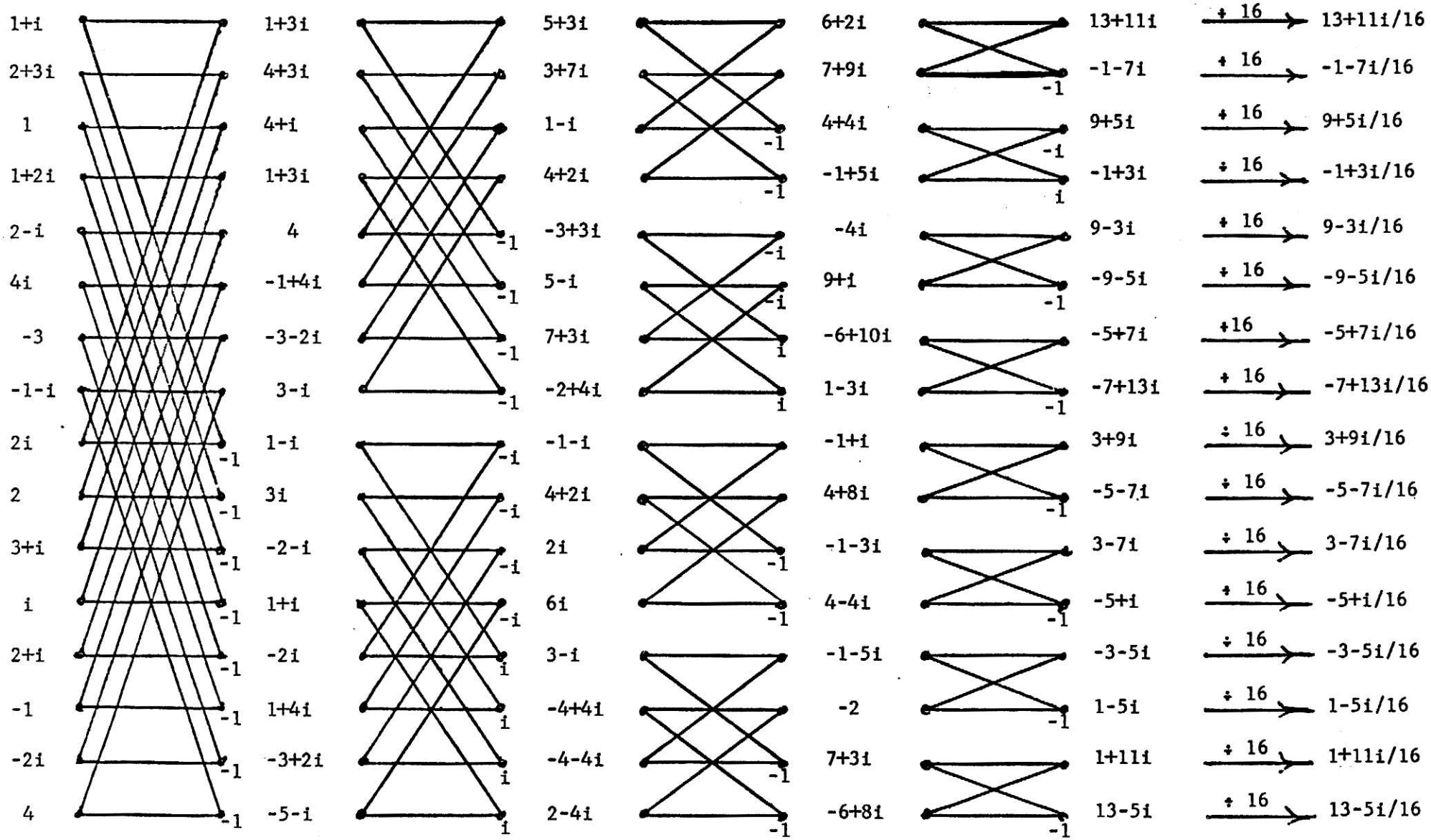

Fig. (2.4). Example illustrating CBT for N = 16.

2.5 Inverse Complex BIFORE Transform (ICBT)

The ICBT yields the original signal or periodic sequence $\boxed{\underline{X}(n)}$ from the transform sequence $\boxed{\underline{B}_X(n)}$.

It is recalled that the CBT is defined as

$$\boxed{\underline{B}_X(n)} = \frac{1}{N} \boxed{H_c(n)} \boxed{\underline{X}(n)} \quad . \tag{2.21}$$

To solve for $\boxed{\underline{X}(n)}$, expression (2.21) is multiplied by $\boxed{H_c^*(n)}^T$ to obtain

$$\boxed{H_c^*(n)}^T \boxed{\underline{B}_X(n)} = \frac{1}{N} \boxed{H_c^*(n)}^T \boxed{H_c(n)} \boxed{\underline{X}(n)} \quad . \tag{2.22}$$

Applying the orthogonal property of $\boxed{H_c(n)}$ in (2.4) to (2.22) there results

$$\boxed{\underline{X}(n)} = \boxed{H_c^*(n)}^T \boxed{\underline{B}_X(n)} \quad . \tag{2.23}$$

AN ALGORITHM TO COMPUTE THE ICBT

The derivation of the algorithm is best illustrated for the case N = 8. Then (2.23) becomes

$$\boxed{\underline{X}(3)} = \boxed{H_c^*(3)}^T \boxed{\underline{B}_X(3)} \quad . \tag{2.24}$$

Substituting for $\boxed{H_c^*(3)}^T$, the transpose of the complex conjugate of $\boxed{H_c(3)}$, the following eight equations are obtained.

$$\begin{aligned}
x(0) &= \{B(0) + B(1)\} + \{B(2) + B(3)\} + \{B(4) + B(5)\} + \{B(6) + B(7)\} \\
x(1) &= \{B(0) - B(1)\} + i\{B(2) - B(3)\} + \{B(4) - B(5)\} + \{B(6) - B(7)\} \\
x(2) &= \{B(0) + B(1)\} - \{B(2) + B(3)\} + i\{B(4) + B(5)\} - i\{B(6) + B(7)\} \\
x(3) &= \{B(0) - B(1)\} - i\{B(2) - B(3)\} + i\{B(4) - B(5)\} - i\{B(6) - B(7)\} \\
x(4) &= \{B(0) + B(1)\} + \{B(2) + B(3)\} - \{B(4) + B(5)\} - \{B(6) + B(7)\} \\
x(5) &= \{B(0) - B(1)\} + i\{B(2) - B(3)\} - \{B(4) - B(5)\} - \{B(6) - B(7)\} \\
x(6) &= \{B(0) + B(1)\} - \{B(2) + B(3)\} - i\{B(4) + B(5)\} + i\{B(6) + B(7)\} \\
x(7) &= \{B(0) - B(1)\} - i\{B(2) - B(3)\} - i\{B(4) - B(5)\} + i\{B(6) - B(7)\} \quad .
\end{aligned} \tag{2.25}$$

The arithmetic operations in (2.25) are summarized in Fig.(2.5).

Iteration 1

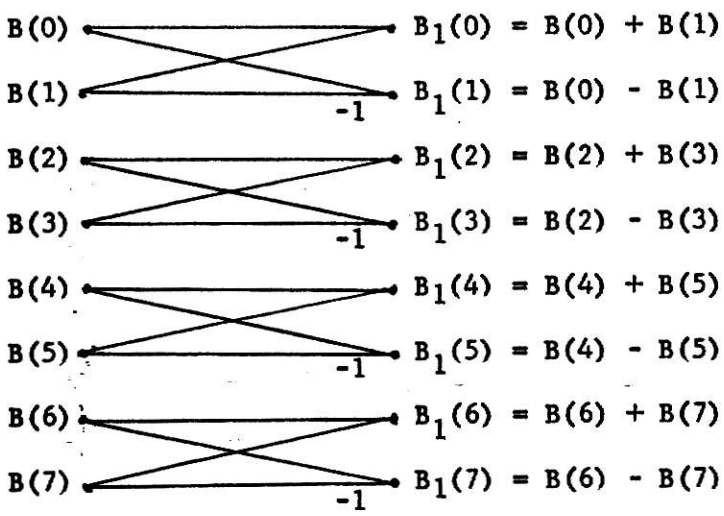

Fig. (2.5). Summary of arithmetic operations in (2.25).

In terms of $B_1(k)$, $k = 0, 1, \ldots 7$, expression (2.25) can be written as

$$
\begin{aligned}
x(0) &= \{B_1(0) + B_1(2)\} + \{B_1(4) + B_1(6)\} \\
x(1) &= \{B_1(1) + iB_1(3)\} + \{B_1(5) + B_1(7)\} \\
x(2) &= \{B_1(0) - B_1(2)\} + i\{B_1(4) + B_1(6)\} \\
x(3) &= \{B_1(1) - iB_1(3)\} + i\{B_1(5) - B_1(7)\} \\
x(4) &= \{B_1(0) + B_1(2)\} - \{B_1(4) + B_1(6)\} \\
x(5) &= \{B_1(1) + iB_1(3)\} - \{B_1(5) + B_1(7)\} \\
x(6) &= \{B_1(0) - B_1(2)\} - i\{B_1(4) - B_1(6)\} \\
x(7) &= \{B_1(1) - iB_1(3)\} - i\{B_1(5) - B_1(7)\} .
\end{aligned}
\tag{2.26}
$$

Figure (2.6) summarizes the arithmetic operations in (2.26).

Iteration 2

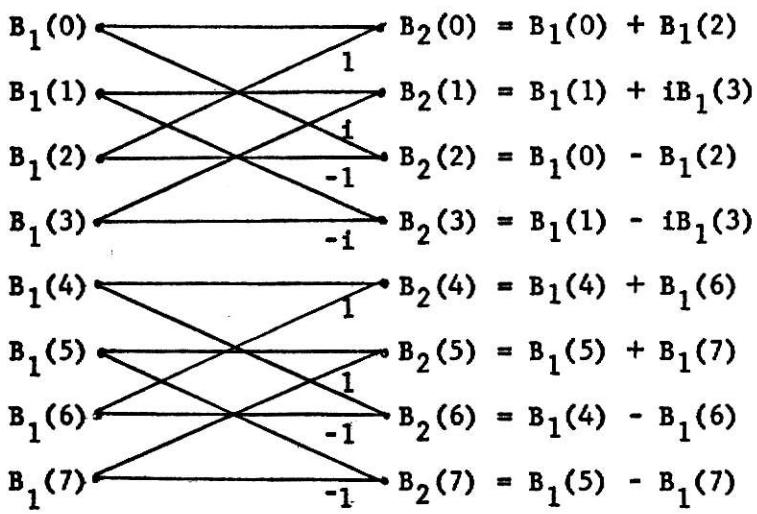

Fig. (2.6). Summary of arthmetic operations in (2.26).

The multipliers used in iteration 2 (see Fig. (2.6))are 1, -1, i and -i. After the second iteration, equations in (2.26) become simpler as written next. Once again (2.26) is written in terms of $B_2(k)$, k = 0, 1, 2, ..., 7 to obtain the following eight equations.

$$
\begin{aligned}
x(0) &= B_2(0) + B_2(4) \\
x(1) &= B_2(1) + B_2(5) \\
x(2) &= B_2(2) + iB_2(6) \\
x(3) &= B_2(3) + iB_2(7) \\
x(4) &= B_2(0) - B_2(4) \\
x(5) &= B_2(1) - B_2(5) \\
x(6) &= B_2(2) - iB_2(6) \\
x(7) &= B_2(3) - iB_2(7) \ .
\end{aligned}
\tag{2.27}
$$

The equations in (2.27) represent third iteration as shown in Fig. (2.7).

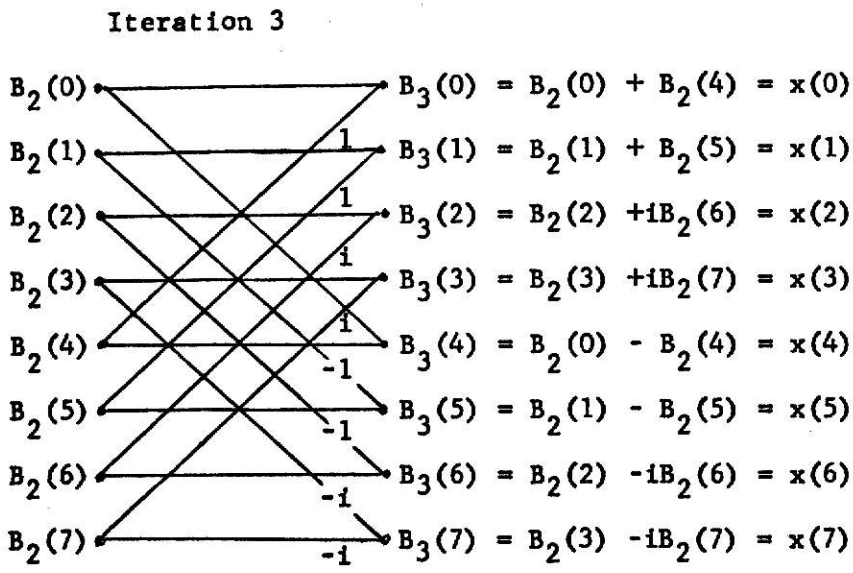

Fig.(2.7). Summary of arithmetic operations in (2.27).

Combining Figs. (2.5), (2.6) and (2.7), one obtains the signal flow graph for N = 8 as shown in Fig. (2.8). The signal flow graph for N = 16 is shown in Fig. (2.9).

From these signal flow graphs, the following observations and generalizations result.

1. In general there are $\log_2 N$ iterations.

2. In the first iteration, $\frac{N}{2}$ pairs of points are added and subtracted to obtain the input to the second iteration.

3. The r^{th} iteration, r = 2, 3, . . ., $\log_2 N$ consists of $N/2^r$ groups with 2^r data points in each group. The first of these groups takes each of the multipliers 1, i, -1, -i for $(2)^{r-2}$ times. Each of the remaining $\frac{N}{2^r - 1}$ groups take the multipliers 1, -1 and hence involve only additions and subtractions.

4. The total number of arithmetic operations required to recover all the N data points x(0), x(1), . . ., x(N-1) is proportional to $N \cdot \log_2 N$.

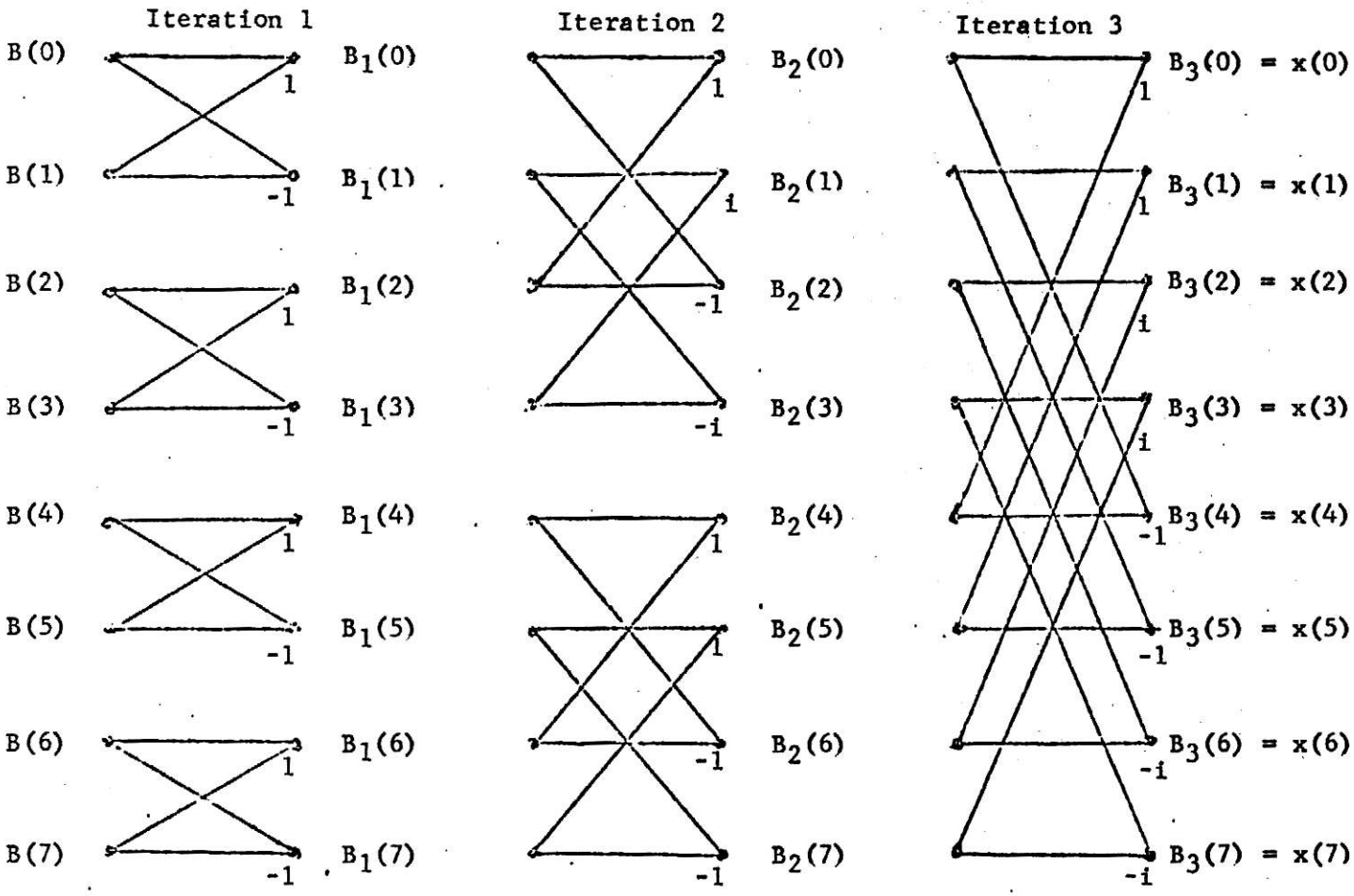

Fig. (2.8). ICBT Signal flow graph, N = 8.

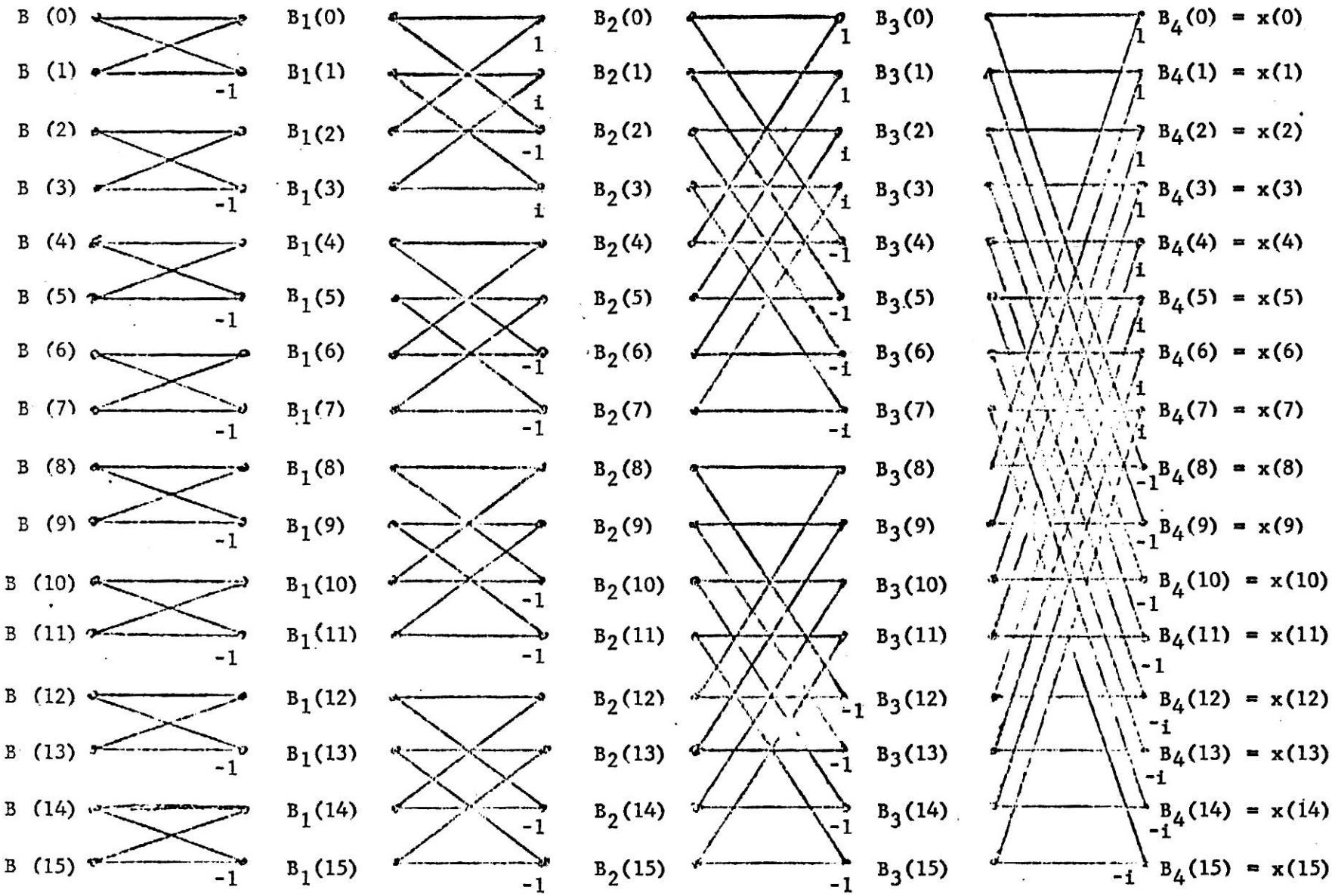

Fig. (2.9). ICBT signal flow graph, N = 16.

In conclusion Fig. (2.10) illustrates the ICBT for the case N = 8 with

$$\left[\underline{B}_x(3)\right]^T = \left[\frac{10+10i}{8}, \frac{-2i}{8}, \frac{-3-i}{8}, \frac{-3+5i}{8}, \frac{1+3i}{8}, \frac{-1-i}{8}, \frac{1+i}{8}, \frac{3-7i}{8}\right] .$$

The corresponding data sequence $\left[\underline{x}(3)\right]$ is seen to be

$$\left[\underline{x}(3)\right]^{NT} = \left[1+i,\ 2+3i,\ 1,\ 1+2i,\ 2i,\ 2,\ 3+i,\ i\right] .$$

Note that the above results are consistent with the numerical example associated with the CBT in Fig. (2.3).

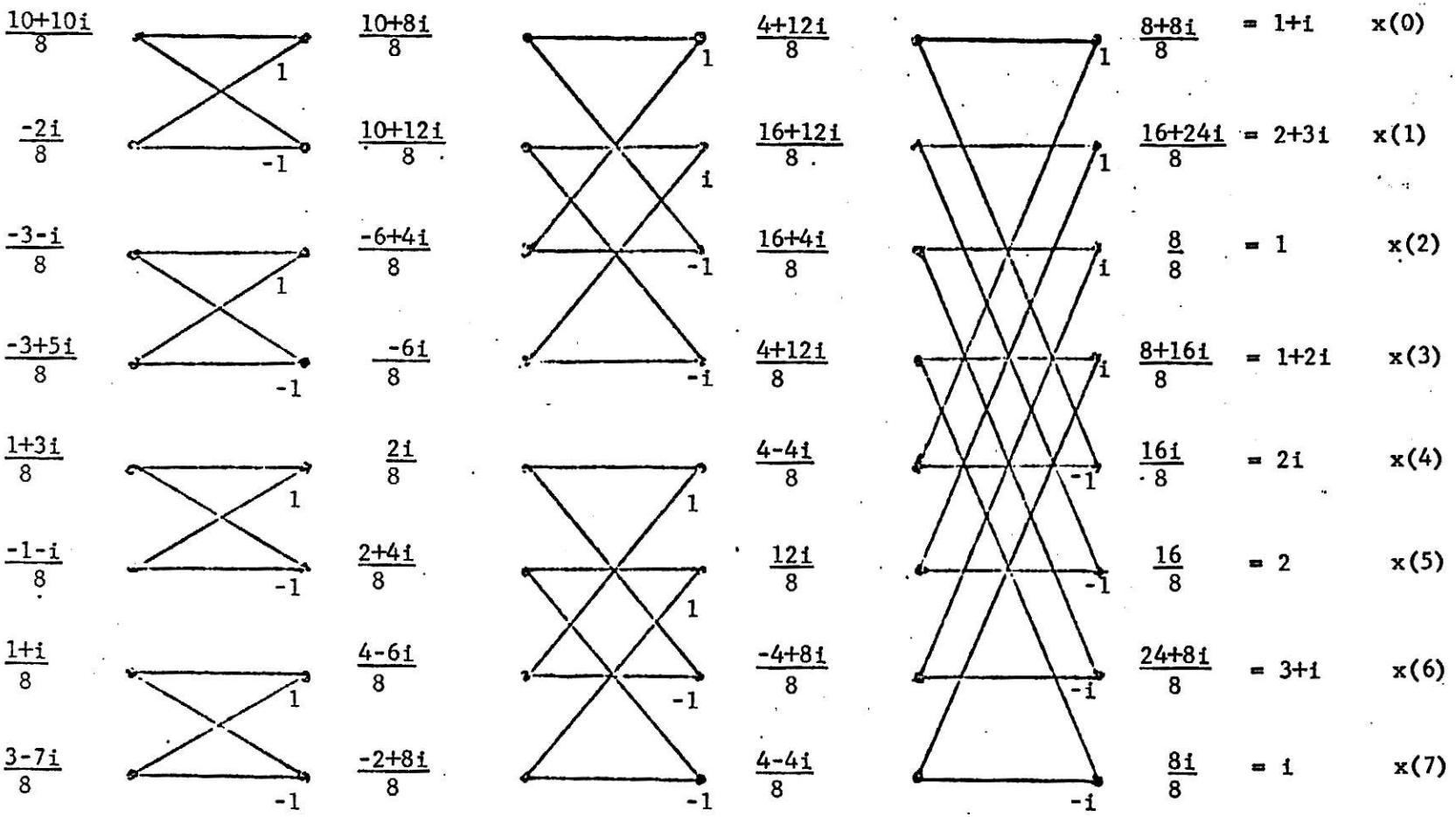

Fig. (2.10) ICBT signal flow graph, 2π example, N = 8.

CHAPTER III

POWER SPECTRUM CONSIDERATIONS

3.1 CBT Shift Matrix

The key to obtaining a power spectrum for the CBT introduced in Chapter I is the shift matrix which relates the CBT coefficients of a shifted sequence to those of the original sequence $[X(n)]$. It is recalled that the CBT is defined as

$$[B_X(n)] = \frac{1}{N}[H_c(n)][X(n)] . \tag{3.1}$$

Let $[X^{(1)}(n)]$ denote the complex N-periodic sequence obtained by shifting the original sequence $[X(n)]$ to the left by one position. Then

$$[X^{(1)}(n)]^T = [x(1) \quad x(2) \quad \ldots \quad x(N-1) \quad x(0)] ,$$

where $[X^{(1)}(n)]^T$ is the vector representation of $[X^{(1)}(n)]$.

Using matrix notation, $[X(n)]$ and $[X^{(1)}(n)]$ are related as follows

$$[X^{(1)}(n)] = [M(n)][X(n)] \tag{3.2}$$

where

$$[M(n)] = \begin{bmatrix} 0 & 1 & 0 & 0 & 0 & 0 & 0 & 0 \\ 0 & 0 & 1 & 0 & 0 & 0 & 0 & 0 \\ 0 & 0 & 0 & 1 & 0 & 0 & 0 & 0 \\ 0 & 0 & 0 & 0 & 1 & 0 & 0 & 0 \\ 0 & 0 & 0 & 0 & 0 & 1 & 0 & 0 \\ 0 & 0 & 0 & 0 & 0 & 0 & 1 & 0 \\ 0 & 0 & 0 & 0 & 0 & 0 & 0 & 1 \\ 1 & 0 & 0 & 0 & 0 & 0 & 0 & 0 \end{bmatrix} .$$

If $\left[\underline{B}^{(1)}(n)\right]$ denotes the CBT of $\left[\underline{X}^{(1)}(n)\right]$, then from (3.2) it follows that

$$\left[\underline{B}^{(1)}(n)\right] = \frac{1}{N}\left[H_c(n)\right]\left[\underline{X}^{(1)}(n)\right] . \tag{3.3}$$

Substituting (3.2) in (3.3), there results

$$\left[\underline{B}^{(1)}(n)\right] = \frac{1}{N}\left[H_c(n)\right]\left[M(n)\right]\left[\underline{X}(n)\right] . \tag{3.4}$$

From the ICBT defined in (2.23) and (3.4) if follows that

$$\left[\underline{B}^{(1)}(n)\right] = \frac{1}{N}\left[H_c(n)\right]\left[M(n)\right]\left[H_c^*(n)\right]^T\left[\underline{B}_x(n)\right]$$

or

$$\left[B^{(1)}(n)\right] = \left[A(n)\right]\left[\underline{B}_x(n)\right] \tag{3.5}$$

where

$$\left[A(n)\right] = \frac{1}{N}\left[H_c(n)\right]\left[M(n)\right]\left[H_c^*(n)\right]^T .$$

Clearly $\left[A(n)\right]$ in (3.5) is the desired shift matrix since it relates the CBT of the shifted sequence $\left[\underline{X}^{(1)}(n)\right]$ to the CBT of the original sequence $\left[\underline{X}(n)\right]$.

In particular consider the case N = 8. Then substitution of the element values of $\left[H_c(n)\right]$, $\left[M(n)\right]$ and $\left[H_c^*(n)\right]^T$ in the expression for $\left[A(n)\right]$ in (3.5) results in the following shift matrix

$$\boxed{A(3)} = \begin{bmatrix} 1 & 0 & & & & & & \\ 0 & -1 & & & & & & \\ & & i & 0 & & & & \\ & & 0 & -i & & & & \\ & & & & \frac{1+i}{2} & \frac{-1+i}{2} & & \\ & & & & \frac{1-i}{2} & \frac{-1-i}{2} & & \\ & & & & & & \frac{1-i}{2} & \frac{-1-i}{2} \\ & & & & & & \frac{1+i}{2} & \frac{-1+i}{2} \end{bmatrix} . \qquad (3.6)$$

Inspection of (3.6) results in two observations which concern the following properties of $\boxed{A(3)}$:

(i) $\boxed{A(3)}$ has a block-diagonal structure.

(ii) There are $2 \cdot \log_2 8$ submatrices along the main diagonal (indicated by the partitioning in (3.6)).

(iii) The submatrices mentioned in (ii) are orthonormal.

It can be shown that (see Appendix B) in general, $\boxed{A(n)}$ has $2 \cdot \log_2 N$ orthonormal submatrices which have recursion properties. That is

$$\boxed{A(n)} = \begin{bmatrix} A_1(0) & & & & & & \\ & A_2(0) & & & & & \\ & & C_1(0) & & & & \\ & & & C_2(0) & & & \\ & & & & C_1(1) & & \\ & & & & & C_2(1) & \\ & & & & & & \ddots \\ & & & & & & C_1(n-2) \\ & & & & & & & C_2(n-2) \end{bmatrix} \qquad (3.7)$$

where $n = \log_2 N$,

$$\boxed{A_1(0)} = \boxed{1}$$

$$\boxed{A_2(0)} = \boxed{-1}$$

$$\boxed{C_2(k)} = \boxed{C_1^*(k)} \quad \text{for } k = 0, 1, 2, \ldots, (n-2).$$

$$\boxed{C_m(k)} = \boxed{H(k)} \left[\boxed{M(k)} - \boxed{U(k)} + (-1)^{m+1} i \boxed{U(k)} \right] \boxed{H(k)} ,$$

for $k = 0, 1, 2, \ldots, (n-2)$; and $m = 1, 2$, and $\boxed{U(k)}$ is defined in Appendix B. In what follows, the shift matrix developed above will be used to obtain the CBT power spectrum.

3.2 CBT Power Spectrum

In Fourier Analysis, it is well known that the power spectrum is invariant with respect to shifts in the signal. This is a fundamental property of a power spectrum. A CBT power spectrum which has this shift invariant property will be developed in what follows.

Consider the case N = 8. Then from (3.5) and (3.6), it follows that

$$\begin{bmatrix} B^{(1)}(0) \\ B^{(1)}(1) \\ B^{(1)}(2) \\ B^{(1)}(3) \\ B^{(1)}(4) \\ B^{(1)}(5) \\ B^{(1)}(6) \\ B^{(1)}(7) \end{bmatrix} = \begin{bmatrix} A_1(0) & & & & & & & \\ & A_2(0) & & & & & & \\ & & C_1(0) & & & & & \\ & & & C_2(0) & & & & \\ & & & & C_1(1) & & & \\ & & & & & C_2(1) & & \\ & & & & & & \bigcirc & \\ & & & & & & & \bigcirc \end{bmatrix} \begin{bmatrix} B(0) \\ B(1) \\ B(2) \\ B(3) \\ B(4) \\ B(5) \\ B(6) \\ B(7) \end{bmatrix} \tag{3.8}$$

where

$$\boxed{A_1(0)} = \boxed{1}$$

$$\boxed{A_2(0)} = \boxed{-1}$$

$$\boxed{C_1(0)} = \boxed{i}$$

$$\boxed{C_2(0)} = \boxed{-i}$$

$$\left[C_1(1)\right] = \begin{bmatrix} \frac{1+i}{2} & \frac{-1+i}{2} \\ \frac{1-i}{2} & \frac{-1-i}{2} \end{bmatrix}$$

and

$$\left[C_2(1)\right] = \begin{bmatrix} \frac{1-i}{2} & \frac{-1-i}{2} \\ \frac{1+i}{2} & \frac{-1+i}{2} \end{bmatrix} .$$

Using elementary matrix partitioning, (3.8) yields

$$\begin{aligned} B^{(1)}(0) &= B(0) \\ B^{(1)}(1) &= -B(1) \\ B^{(1)}(2) &= iB(2) \\ B^{(1)}(3) &= -iB(3) \\ \begin{bmatrix} B^{(1)}(4) \\ B^{(1)}(5) \end{bmatrix} &= \left[C_1(1)\right] \begin{bmatrix} B(4) \\ B(5) \end{bmatrix} \end{aligned}$$

and

$$\begin{bmatrix} B^{(1)}(6) \\ B^{(1)}(7) \end{bmatrix} = \left[C_2(1)\right] \begin{bmatrix} B(6) \\ B(7) \end{bmatrix} . \qquad (3.9)$$

Since the matrices $\left[C_1(1)\right]$ and $\left[C_2(1)\right]$ are orthonormal, from (3.9), it follows that

$$\begin{aligned} \left|B^{(1)}(0)\right|^2 &= \left|B(0)\right|^2 \\ \left|B^{(1)}(1)\right|^2 &= \left|B(1)\right|^2 \\ \left|B^{(1)}(2)\right|^2 &= \left|B(2)\right|^2 \\ \left|B^{(1)}(3)\right|^2 &= \left|B(3)\right|^2 \\ \sum_{j=4}^{5} \left|B^{(1)}(j)\right|^2 &= \sum_{j=4}^{5} \left|B(j)\right|^2 \end{aligned}$$

and

$$\sum_{j=6}^{7} \left|B^{(1)}(j)\right|^2 = \sum_{j=6}^{7} \left|B(j)\right|^2 . \qquad (3.10)$$

Thus the invariants for one shift in the data sequence $\lceil X(3) \rceil$ are:

$$\begin{aligned} P(0) &= |B(0)|^2 \\ P(1) &= |B(1)|^2 \\ P(2) &= |B(2)|^2 \\ P(3) &= |B(3)|^2 \\ P(4) &= \sum_{j=4}^{5} |B(j)|^2 \\ P(5) &= \sum_{j=6}^{7} |B(j)|^2 \,. \end{aligned} \tag{3.11}$$

However, using the property that powers of orthonormal matrices are also orthonormal, it follows that the above analysis is valid for all 'k' shifts of the data sequence $\lceil X(3) \rceil$ where, k = 0, 1, 2, . . ., 7. Thus the CBT power spectrum for N = 8 is given by the P(i), i = 0, 1, 2, . . ., 5 in (3.11). It is observed that the spectrum has $2 \cdot \log_2 8 = 6$ spectrum points.

In general, it can be shown that the CBT power spectrum has $2 \cdot \log_2 N$ spectrum points which can be defined as follows:

$$\begin{aligned} P(0) &= |B(0)|^2 \\ P(1) &= |B(1)|^2 \\ P(2s+2) &= \sum_{k=2^{s+1}}^{3\cdot 2^{s}-1} |B(k)|^2 \end{aligned} \tag{3.12}$$

and

$$P(2s+3) = \sum_{k=3\cdot 2^{s}}^{2^{s+2}-1} |B(k)|^2 \quad ; \quad s = 1, 2, \ldots, (n-2).$$

If the CBT power spectrum for a real periodic sequence is found, then it is observed that

$$P(0) = |B(0)|^2$$

$$P(1) = |B(1)|^2$$

and $P(2s+2) = P(2s+3)$

where $P(2s+2)$ is given by (3.12).

Figures (3.1) and (3.2) illustrate the computations involved to compute the CBT power spectrum for an 8-periodic and a 16-periodic sequence respectively. From (3.12), it follows that the power spectrum for the 8-periodic sequence in Fig. (3.1) is given by

$$\begin{aligned} P(0) &= 200/64 \\ P(1) &= 4/64 \\ P(2) &= 10/64 \\ P(3) &= 34/64 \\ P(4) &= 12/64 \end{aligned} \qquad (3.13)$$

and $P(5) = 60/64$.

Similarly the power spectrum for the 16-periodic sequence in Fig. (3.2) is given by

$$\begin{aligned} P(0) &= 290/256 \\ P(1) &= 50/256 \\ P(2) &= 106/256 \\ P(3) &= 10/256 \\ P(4) &= 196/256 \\ P(5) &= 292/256 \\ P(6) &= 248/256 \end{aligned} \qquad (3.14)$$

and $P(7) = 376/256$.

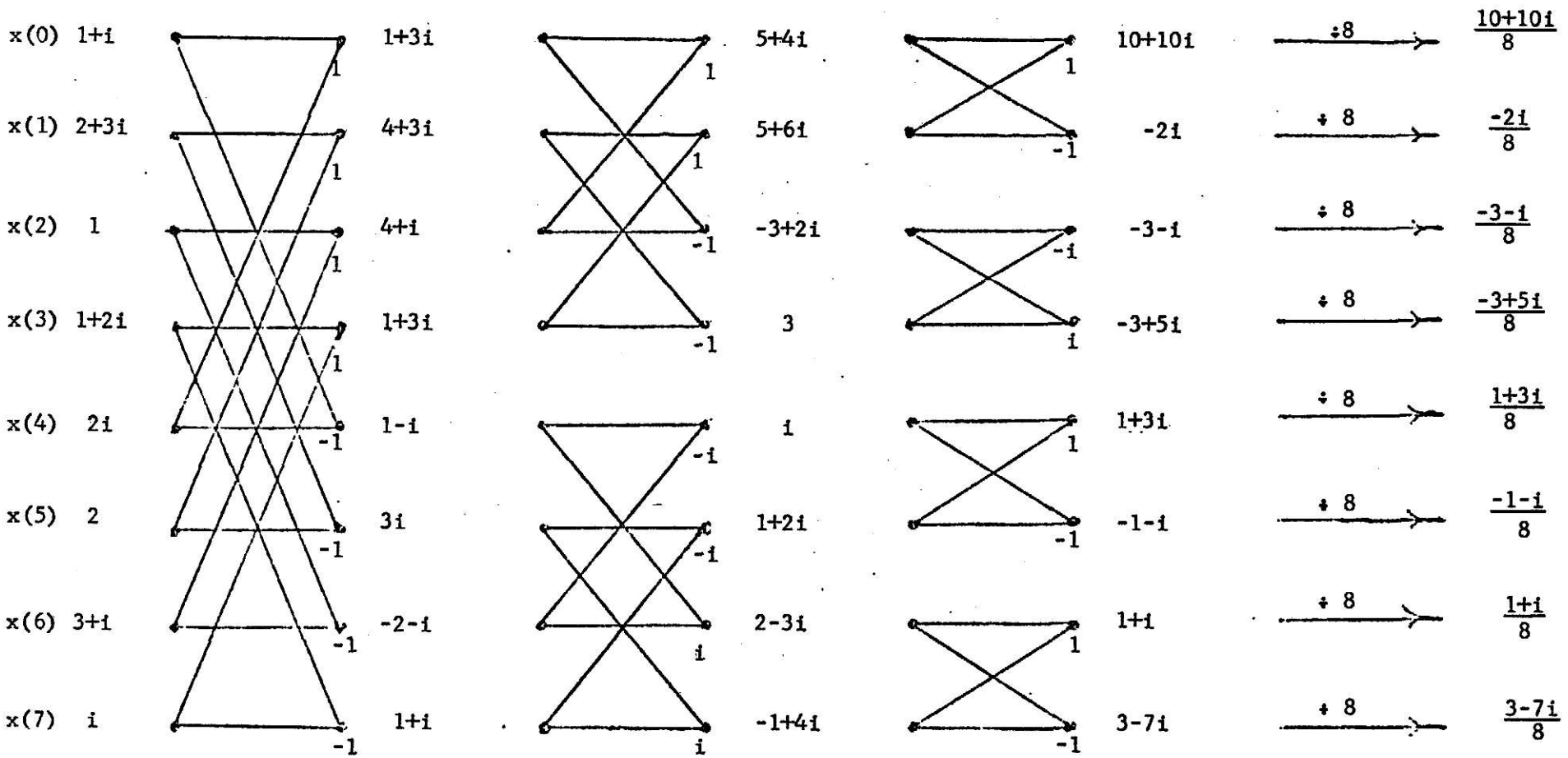

Fig. (3.1). Example illustrating the CBT for 8-periodic sequence.

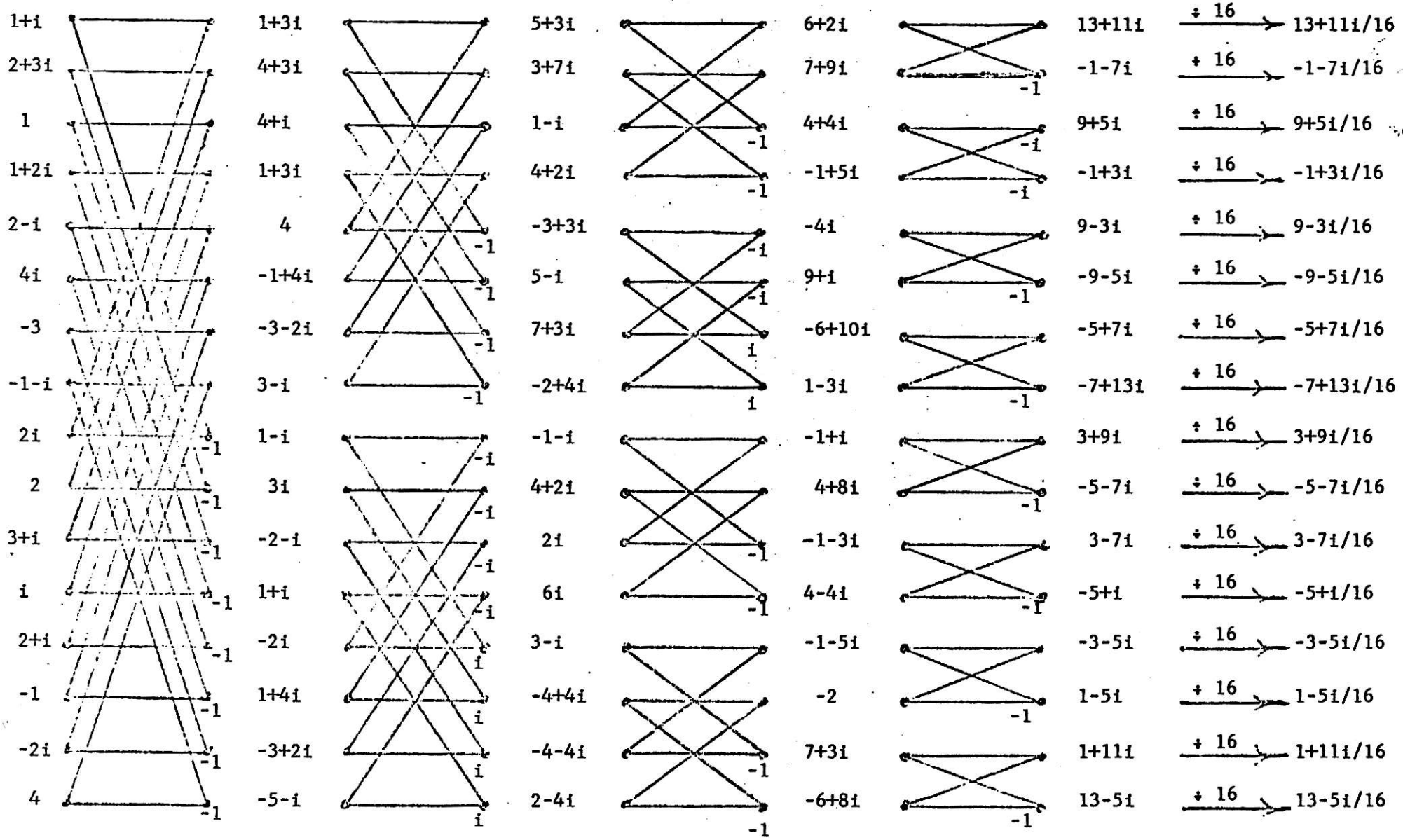

Fig.(3.2). Example illustrating CBT for N = 16.

The number of independent power spectrum points associated with the BT, CBT, and the DFT corresponding to real and complex N-periodic input sequences are summarized in Table (3.1).

Table (3.1)

Name of transform	No. of independent spectrum points	
	real input	complex input
BIFORE	$\log_2 N + 1$	$\log_2 N + 1$
Complex BIFORE	$\log_2 N + 1$	$2 \cdot \log_2 N$
Discrete Fourier	$\frac{N}{2} + 1$	N

3.3 Further Computational Considerations

From (3.12) it is clear that to obtain the CBT power spectrum, it is necessary to compute all the CBT coefficients $B(k)$, $k = 0, 1, 2, \ldots, (N-1)$. In this section it is shown that one can compute the spectrum points directly without first obtaining the transform coefficients. The method is best illustrated for the case $N = 8$.

For $N = 8$, the spectrum points are (see 3.11).

$$P(k) = \left|B(k)\right|^2 , \quad k = 0, 1, 2, 3 . \tag{3.15}$$

However from the signal flow graph $N = 8$ in Fig. (3.1), one has

$$B(k) = \frac{1}{8} x_3(k), \quad k = 0, 1, 2, 3 . \tag{3.16}$$

Combining (3.15) and (3.16) there results

$$P(k) = \frac{\left|x_3(k)\right|^2}{8^2} , \; k = 0, 1, 2, 3 . \tag{3.17}$$

Again examination of the signal flow graph $N = 8$ in Fig. (3.1) reveals that

$$\begin{bmatrix} B(4) \\ B(5) \end{bmatrix} = \frac{1}{8} \begin{bmatrix} 1 & 1 \\ 1 & -1 \end{bmatrix} \begin{bmatrix} x_2(4) \\ x_2(5) \end{bmatrix} \tag{3.18}$$

and
$$\begin{bmatrix} B(6) \\ B(7) \end{bmatrix} = \frac{1}{8} \begin{bmatrix} 1 & 1 \\ 1 & -1 \end{bmatrix} \begin{bmatrix} x_2(6) \\ x_2(7) \end{bmatrix} . \tag{3.19}$$

Taking the transpose and complex conjugate of (3.18), one has

$$\begin{bmatrix} B^*(4) & B^*(5) \end{bmatrix} = \frac{1}{8} \begin{bmatrix} x_2^*(4) & x_2^*(5) \end{bmatrix} \begin{bmatrix} 1 & 1 \\ 1 & -1 \end{bmatrix} . \tag{3.20}$$

Multiplication of (3.18) and (3.20) results in

$$\begin{bmatrix} B^*(4) & B^*(5) \end{bmatrix} \begin{bmatrix} B(4) \\ B(5) \end{bmatrix} = \frac{1}{8^2} \begin{bmatrix} x_2^*(4) & x_2^*(5) \end{bmatrix} \begin{bmatrix} 1 & 1 \\ 1 & -1 \end{bmatrix} \begin{bmatrix} 1 & 1 \\ 1 & -1 \end{bmatrix} \begin{bmatrix} x_2(4) \\ x_2(5) \end{bmatrix}$$

or
$$\begin{bmatrix} |B(4)|^2 + |B(5)|^2 \end{bmatrix} = \frac{2}{8^2} \begin{bmatrix} |x_2(4)|^2 + |x_2(5)|^2 \end{bmatrix} . \tag{3.21}$$

The left hand side of (3.21) is precisely P(4) (see (3.11)).

Hence (3.21) can be written as

$$P(4) = \frac{2}{8^2} \sum_{k=4}^{5} |x_2(k)|^2 . \tag{3.22}$$

A similar treatment of (3.19) yields

$$P(5) = \frac{2}{8^2} \sum_{k=6}^{7} |x_2(k)|^2 . \tag{3.23}$$

The arithmetic operations in (3.17), (3.22) and (3.23) which yield the power spectrum are summarized in the flow graph shown in Fig. (3.3). From this flow graph it follows that its general version consists of $\log_2 N$ iterations. The r^{th} iteration yields 2^{r-1} groups with $N/2^{r-1}$ data points in each group for r = 1, 2, 3, . . ., n. The data points in each of the lower group yields two spectrum points. Thus the general form of (3.17), (3.22) and (3.23) can be expressed as follows:

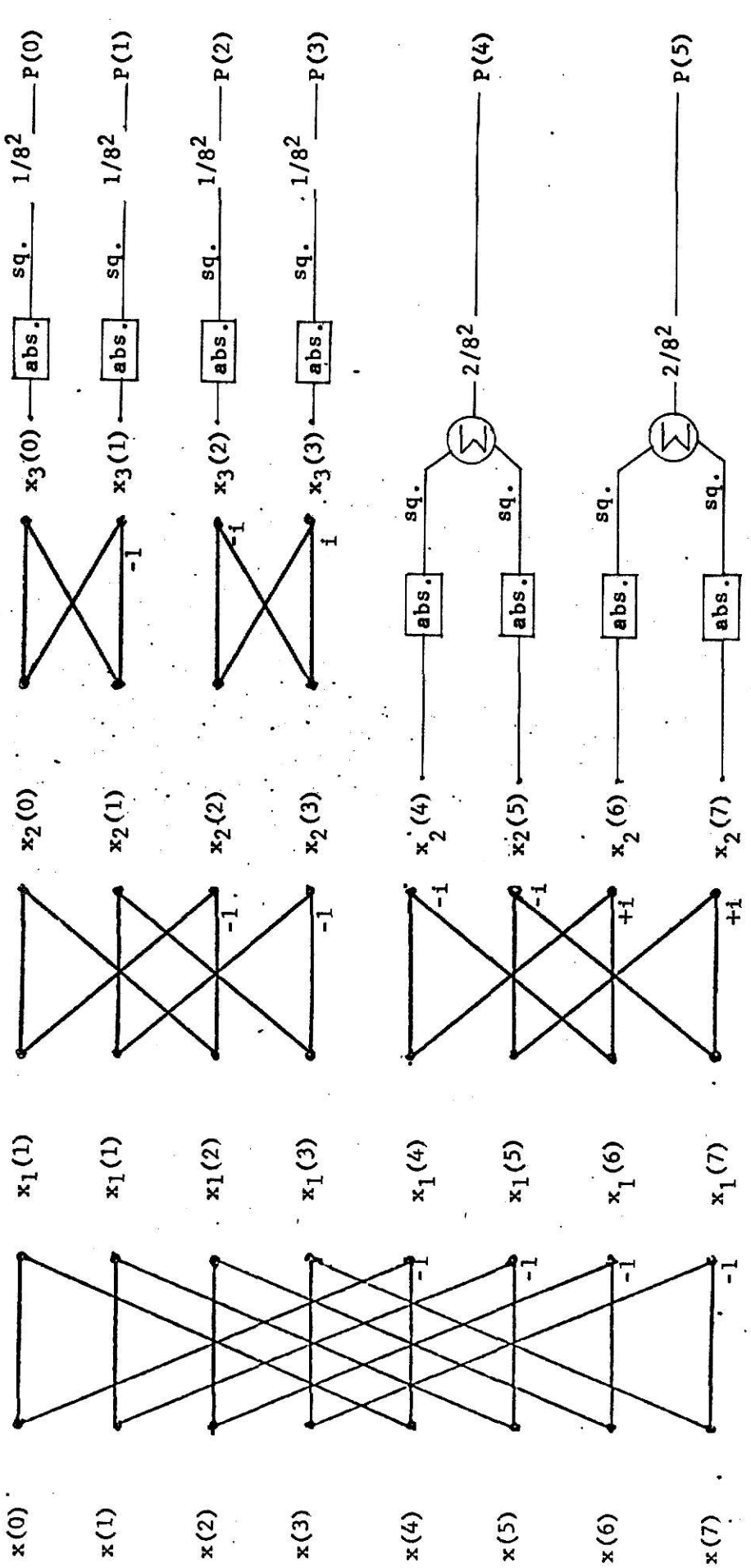

Fig. (3.3). Signal flow graph of CBT power spectrum for N = 8.

$$P(k) = \frac{1}{N^2} \left| x_n(k) \right|^2 \quad , k = 0, 1, 2, 3$$

$$P(2s+2) = \frac{2^s}{N^2} \sum_{k=2^{s+1}}^{3\cdot 2^s - 1} \left| x_{n-s}(k) \right|^2$$

and

$$P(2s+3) = \frac{2^s}{N^2} \sum_{k=3\cdot 2^s}^{2^{s+2}-1} \left| x_{n-s}(k) \right|^2 \qquad (3.24)$$

for $s = 1, 2, 3, \ldots, (n-2)$.

where $n = \log_2 N$

and $x_r(k)$ denotes the k^{th} output data point of the r^{th} iteration, $r = 1, 2, \ldots, n$.

Based on (3.24) the power spectrum for a 16-periodic sequence is derived and is shown in Fig. (3.4).

In conclusion, two numerical examples for the cases N = 8 and N = 16 in (3.24) are included in Fig. (3.5) and Fig. (3.6) respectively. From Fig. (3.5), the CBT power spectrum of the 8-periodic sequence shown is given by

$$P(0) = 200/64$$
$$P(1) = 4/64$$
$$P(2) = 10/64$$
$$P(3) = 34/64 \qquad (3.25)$$
$$P(4) = 12/64$$

and $P(5) = 60/64$.

Again, the power spectrum of the 16-periodic sequence shown in Fig. (3.6) is given by

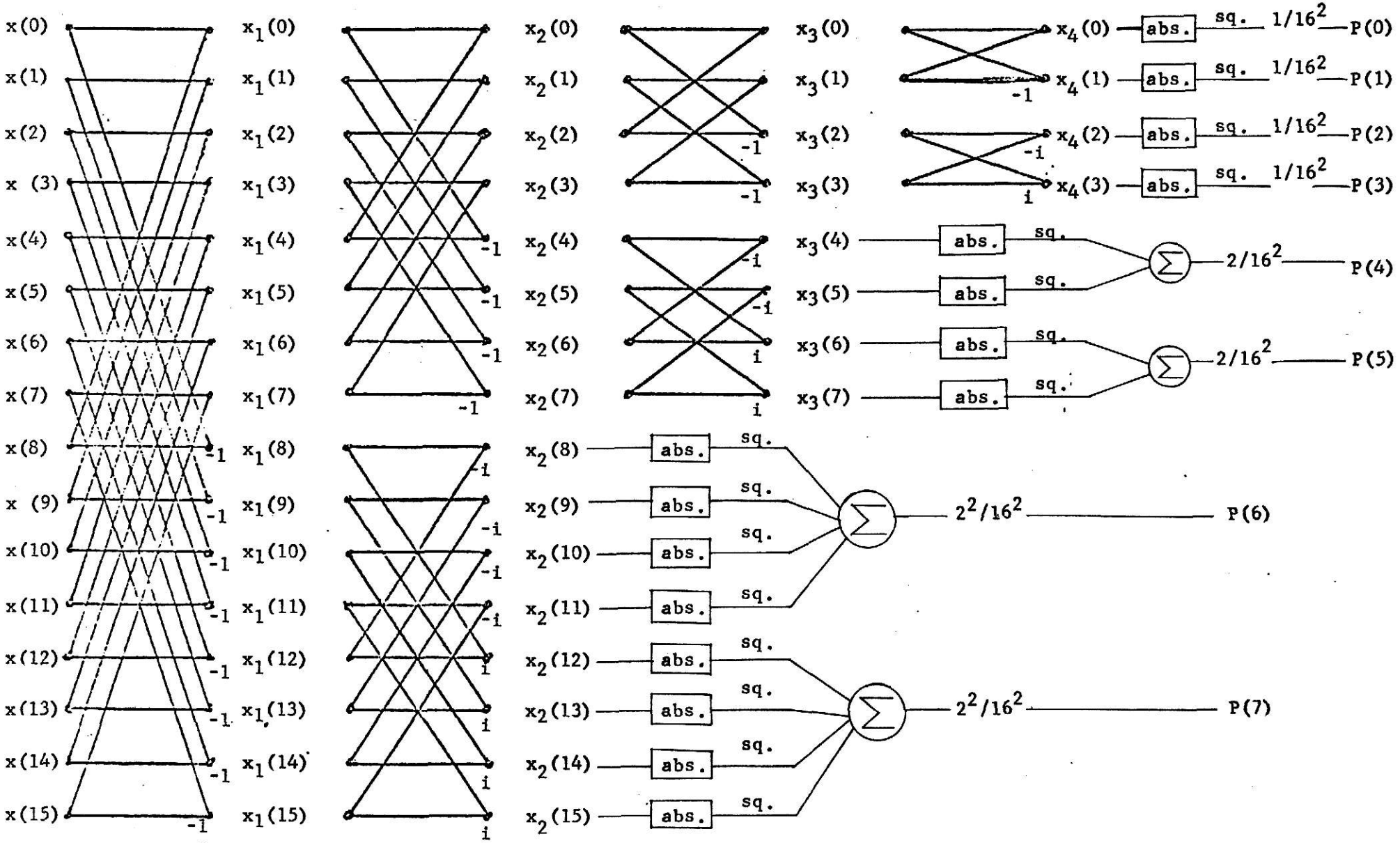

Fig. (3.4). Signal flow graph of CBT power spectrum for N = 16.

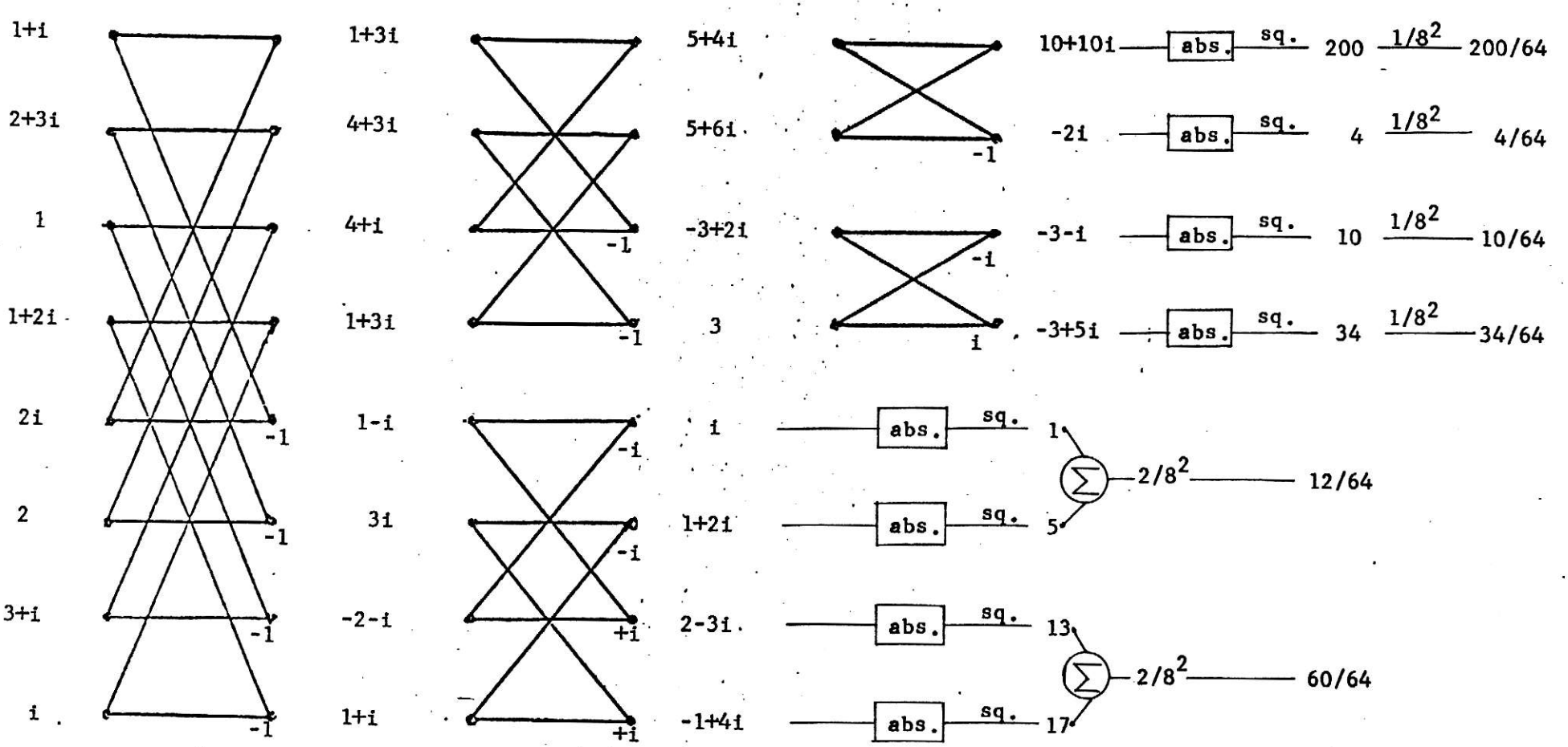

Fig. (3.5). Example of CBT power spectrum for N = 8.

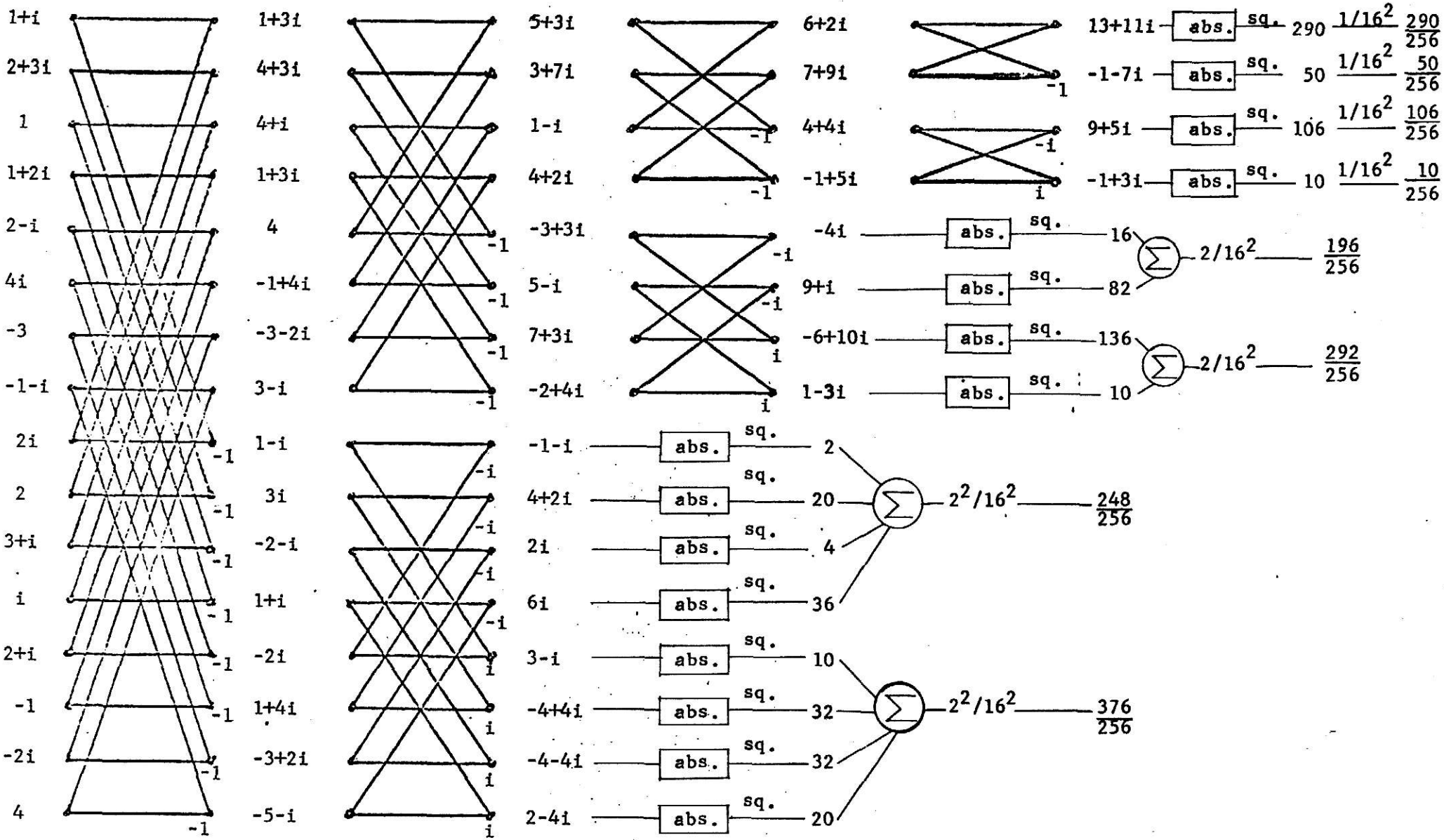

Fig. (3.6). Example of CBT power spectrum for N = 16.

$$
\begin{aligned}
P(0) &= 290/256 \\
P(1) &= 50/256 \\
P(2) &= 106/256 \\
P(3) &= 10/256 \\
P(4) &= 196/256 \\
P(5) &= 292/256 \\
P(6) &= 248/256 \\
P(7) &= 376/256 .
\end{aligned}
\tag{3.26}
$$

3.4 Autocorrelation Theorem

The cross-correlation sequence of two real N-periodic sequences $[x(n)]$ and $[y(n)]$ is defined as

$$[z(k)] = \frac{1}{N} \sum_{h=0}^{N-1} x(h) \cdot y(k+h) \tag{3.27}$$

for k = 0, 1, 2, . . ., (N-1).

If $[y(n)]$ and $[x(n)]$ are identical, then (3.27) represents the auto correlation sequence and is defined as

$$[z(k)] = \frac{1}{N} \sum_{h=0}^{N-1} x(h) \cdot x(k+h) \tag{3.28}$$

for k = 0, 1, 2, . . ., (N-1).

In the case of the real BIFORE transform Ohnsorg [3] has shown that the BT power spectrum can be computed from the BT coefficients of $[z(k)]$ in (3.28), as follows:

$$P(o) = B_z(0)$$

and

$$P(s) = \sum_{k=2^{s-1}}^{2^s-1} B_z(k), \quad s = 1, 2, \ldots, n \tag{3.29}$$

where, $B_z(k)$, $k = 0, 1, 2, \ldots, (N-1)$ are the BT coefficients of $\boxed{Z(k)}$.

The autocorrelation theorem analogus to that in (3.29) is now considered for the CBT when the input sequence $\boxed{X(n)}$ is complex. Then (3.28) is modified to obtain.

$$\boxed{Z(k)} = \frac{1}{N} \sum_{h=0}^{N-1} x(h) \quad x^*(k+h) \tag{3.30}$$

for $k = 0, 1, 2, \ldots, (N-1)$., and where $x^*(\ )$ is the complex conjugate of $x(\ )$.

The autocorrelation theorem is best demonstrated by means of a numerical example for the case $N = 8$. With $N = 8$, the matrix form of (3.30) is given by

$$\begin{bmatrix} Z(0) \\ Z(1) \\ Z(2) \\ Z(3) \\ Z(4) \\ Z(5) \\ Z(6) \\ Z(7) \end{bmatrix} = \begin{bmatrix} x(0) & x(1) & x(2) & \cdots & x(7) \\ x(7) & x(0) & x(1) & \cdots & x(6) \\ x(6) & x(7) & x(0) & \cdots & x(5) \\ \cdots & \cdots & \cdots & \cdots & \cdots \\ \cdots & \cdots & \cdots & \cdots & \cdots \\ \cdots & \cdots & \cdots & \cdots & \cdots \\ \cdots & \cdots & \cdots & \cdots & \cdots \\ x(1) & x(2) & \cdots & \cdots & x(0) \end{bmatrix} \begin{bmatrix} x^*(0) \\ x^*(1) \\ x^*(2) \\ x^*(3) \\ x^*(4) \\ x^*(5) \\ x^*(6) \\ x^*(7) \end{bmatrix} \tag{3.31}$$

Again, consider the 8-periodic sequence $\boxed{X(3)}$, such that

$$x(0) = 1+i, \quad x(1) = 2+3i, \quad x(2) = 1, \quad x(3) = 1+2i$$
$$x(4) = 2i, \quad x(5) = 2, \quad x(6) = 3+i, \quad x(7) = i \quad , \tag{3.32a}$$

then (3.31) yields

$$Z(0) = 40/8, \quad Z(1) = \frac{20-20i}{8}, \quad Z(2) = \frac{20+6i}{8}, \quad Z(3) = \frac{29-8i}{8}$$

$$Z(4) = \frac{22}{8}, \quad Z(5) = \frac{29+8i}{8}, \quad Z(6) = \frac{20-6i}{8}, \quad Z(7) = \frac{20+2i}{8} \quad . \qquad (3.32b)$$

The signal flow graph which yields the CBT of the sequence $\boxed{Z(3)}$ in (3.32b) is shown in Fig. (3.7).

From Fig. (3.7), one has

$$\begin{aligned} B(0) &= 200/64 \quad , \quad B(1) = 4/64 \\ B(2) &= 34/64 \quad , \quad B(3) = 10/64 \\ B(4) &= \frac{11-19i}{64} \quad , \quad B(5) = \frac{49+19i}{64} \\ B(6) &= \frac{7-i}{64} \quad , \quad B(7) = \frac{5+i}{64} \quad . \end{aligned} \qquad (3.33)$$

Now referring to (3.25), it is found that the CBT power spectrum for the sequence $\boxed{X(3)}$ in (3.32a) is given by

$$\begin{aligned} P(0) &= 200/64 \\ P(1) &= 4/64 \\ P(2) &= 10/64 \\ P(3) &= 34/64 \\ P(4) &= 12/64 \\ P(5) &= 60/64 \quad . \end{aligned} \qquad (3.34)$$

Comparing (3.33) and (3.34), there results

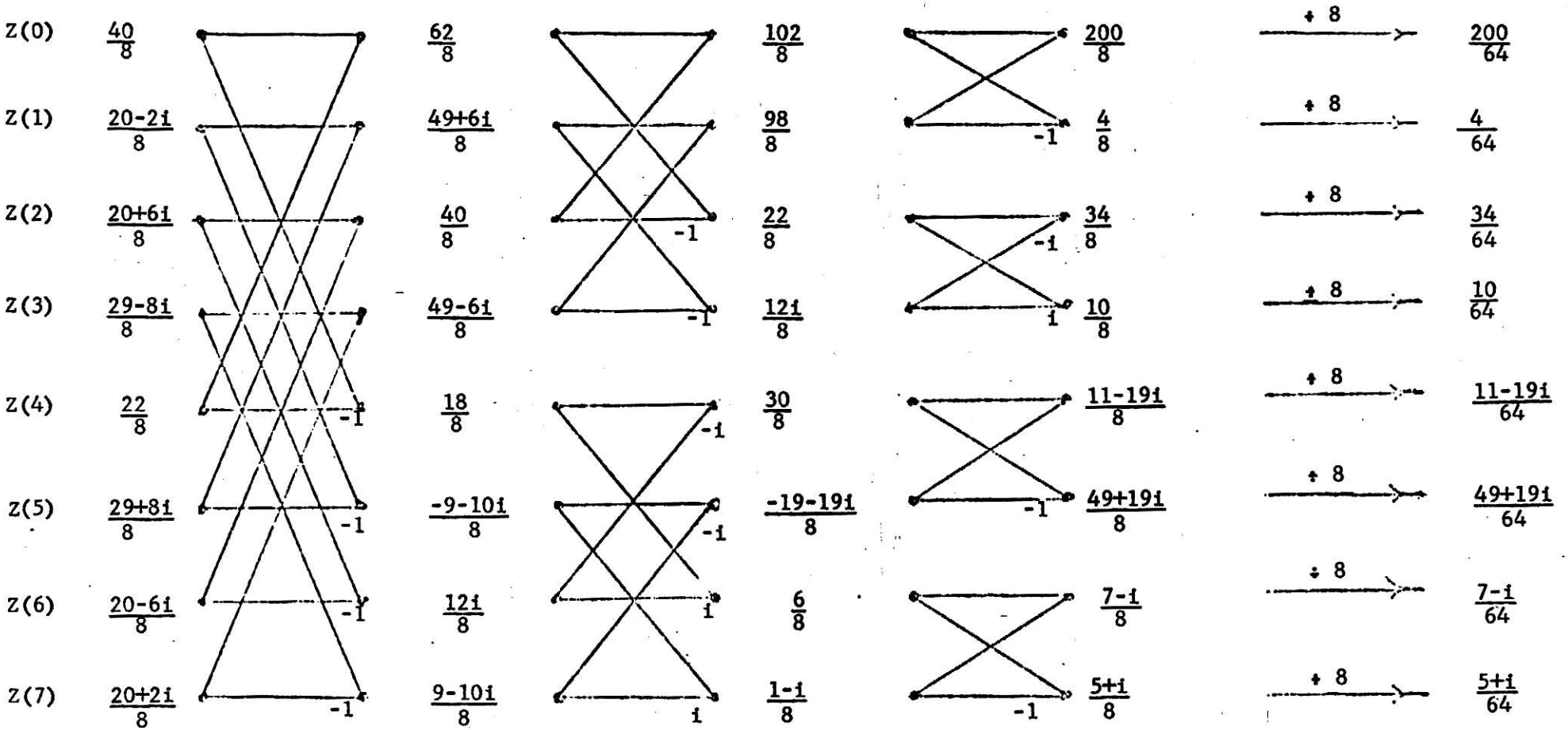

Fig. (3.7). CBT of the autocorrelation sequence.

$$P(0) = B(0)$$

$$P(1) = B(1)$$

$$P(2) = B(3)$$

$$P(3) = B(2)$$

and $$P(4) = B(6) + B(7) \qquad (3.35)$$

$$P(5) = B(4) + B(5) \ .$$

It can be shown that (3.35) generalizes to

$$P(k) = B(k), \quad k = 0, 1$$

$$P(2s+2) = \sum_{m=3\cdot 2^{s}}^{2^{s+2}-1} B(m) \qquad (3.36)$$

$$P(2s+3) = \sum_{m=2^{s+1}}^{3\cdot 2^{s}-1} B(m)$$

for $s = 0, 1, 2, \ldots, (n-2)$ and $n = \log_2 N$.

From (3.36), it is clear that the CBT power spectrum can be obtained from the CBT of the autocorrelation sequence of the input sequence $[X(n)]$. Thus (3.36) is the desired autocorrelation theorem for the CBT.

CHAPTER IV

PHYSICAL INTERPRETATION OF THE CBT POWER SPECTRUM

4.1 Introductory Remarks

In the case of the real BT, there are $(\log_2 N+1)$ power spectrum points. Each spectrum point represents the power in a subsequence which is obtained by decomposing the original input sequence. The input sequence is decomposed into $(\log_2 N+1)$ subsequences which are mutually orthogonal to one another. In this chapter an analogous development is carried out for the CBT.

4.2 A Decomposition Technique

In CBT, there are $2\cdot\log_2 N$ spectrum points. Hence the input sequence should be decomposed into $2\log_2 N$ mutually orthogonal subsequences.

Consider the 8-periodic sequence in Fig. (4.1). With respect to Fig. (4.1), it is convenient to introduce the notation

$$\tilde{x}_r(m) = \frac{x_r(m)}{2^r}, \quad r = 1, 2, 3; \; m = 0, 1, 2, \ldots, 7. \qquad (4.1)$$

Then, it can be shown that the original sequence $\boxed{\tilde{X}(3)}$ can be expressed as a sum of the following subsequences $\boxed{G_r(3)}$ which are expressed in terms of the $\tilde{x}_r(m)$ in (4.1):

$$\begin{aligned}
\boxed{G_0(3)} &= \boxed{\tilde{x}_3(0) \quad \tilde{x}_3(0) \quad \tilde{x}_3(0) \quad \ldots \quad \tilde{x}_3(0)} \\
\boxed{G_1(3)} &= \boxed{\tilde{x}_3(1) \quad -\tilde{x}_3(1) \quad \tilde{x}_3(1) \quad -\tilde{x}_3(1) \quad \ldots \quad -\tilde{x}_3(1)} \\
\boxed{G_2(3)} &= \boxed{\tilde{x}_3(2) \quad i\tilde{x}_3(2) \quad -\tilde{x}_3(2) \quad -i\tilde{x}_3(2) \quad \tilde{x}_3(2) \quad i\tilde{x}_3(2) \quad -\tilde{x}_3(2) \quad -i\tilde{x}_3(2)} \\
\boxed{G_3(3)} &= \boxed{\tilde{x}_3(3) \quad -i\tilde{x}_3(3) \quad -\tilde{x}_3(3) \quad i\tilde{x}_3(3) \quad \tilde{x}_3(3) \quad -i\tilde{x}_3(3) \quad -\tilde{x}_3(3) \quad i\tilde{x}_3(3)} \\
\boxed{G_4(3)} &= \boxed{\tilde{x}_2(4) \quad \tilde{x}_2(5) \quad i\tilde{x}_2(4) \quad i\tilde{x}_2(5) \quad -\tilde{x}_2(4) \quad -\tilde{x}_2(5) \quad -i\tilde{x}_2(4) \quad -i\tilde{x}_2(5)} \\
\boxed{G_5(3)} &= \boxed{\tilde{x}_2(6) \quad \tilde{x}_2(7) \quad -i\tilde{x}_2(6) \quad -i\tilde{x}_2(7) \quad -\tilde{x}_2(6) \quad -\tilde{x}_2(7) \quad i\tilde{x}_2(6) \quad i\tilde{x}_2(7)}
\end{aligned} \qquad (4.2)$$

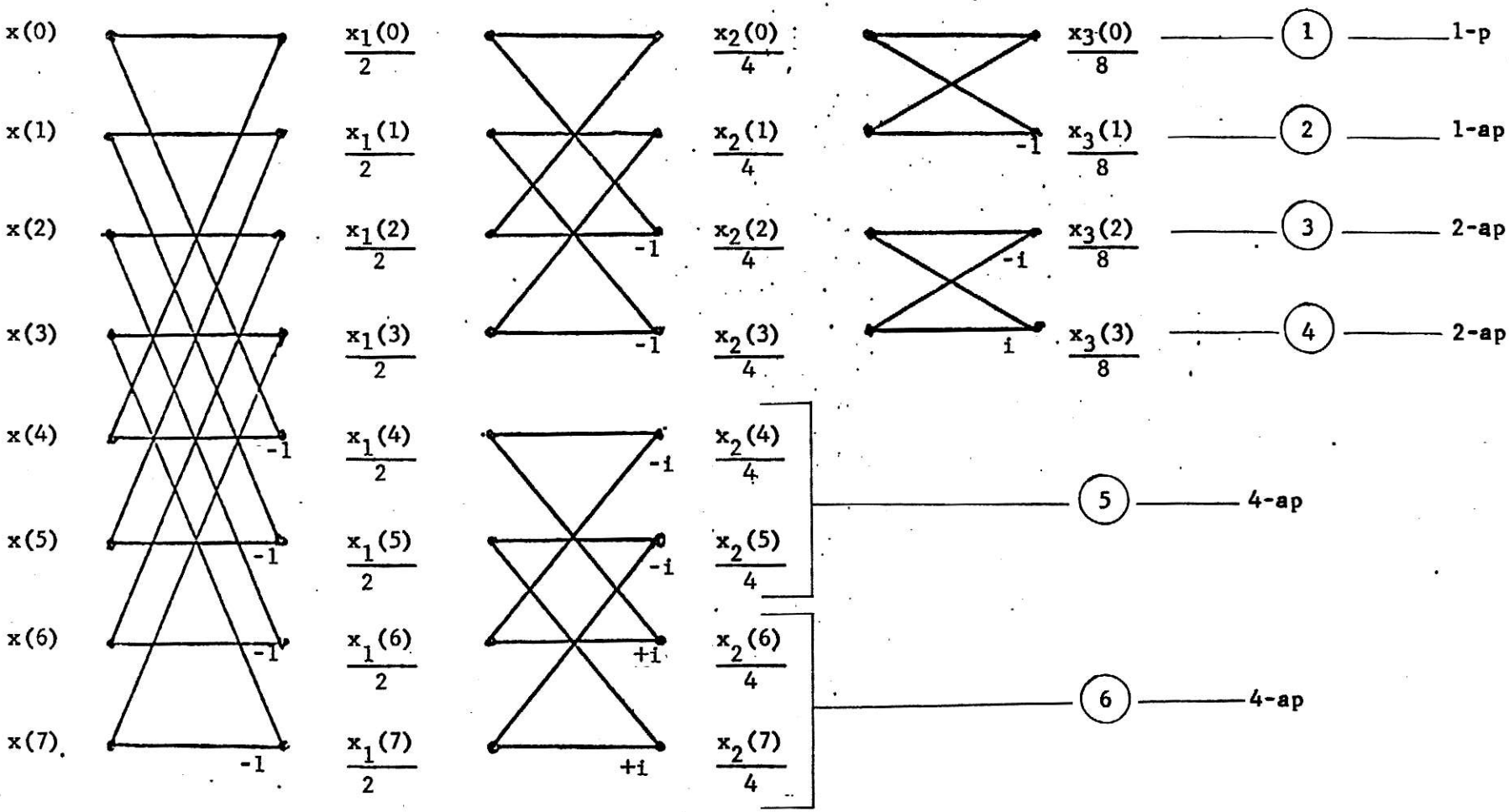

Notation. M-p M-periodic
M-ap M-antiperiodic

Fig. (4.1). Decomposition process, N = 8.

In (4.2), it is observed that:

1. There are 6 i.e., $2\log_2 8$ subsequences $[G_r(3)]$. In general there are $2\log_2 N$ subsequences $[G_r(n)]$, $n = \log_2 N$.

2. $[G_0(3)]$ is 1-periodic, $[G_1(3)]$ is 1-antiperiodic*, $[G_2(3)]$ and $[G_3(3)]$ are 2-antiperiodic and $[G_4(3)]$ and $[G_5(3)]$ are 4-antiperiodic. In general the periodicities of the subsequences $[G_r(n)]$ can be expressed as follows:

$$\begin{aligned} &[G_0(n)] \quad \text{is} \quad \text{1-periodic} \\ &[G_1(n)] \quad \text{is} \quad \text{1-antiperiodic} \end{aligned} \tag{4.3}$$

$[G_{2s+2}(n)]$ and $[G_{2s+3}(n)]$ are 2^{s+1} antiperiodic for $s = 0, 1, 2, \ldots, (n-2)$.

3. The original 8-periodic sequence is given by

$$[X(3)] = \sum_{r=0}^{5} [G_r(3)] \; . \tag{4.4}$$

In general (4.4) can be expressed as

$$[X(n)] = \sum_{r=0}^{2n-1} [G_r(n)]; \quad n = \log_2 N \; . \tag{4.5}$$

A numerical example is considered next. Let

$$[X(3)]^T = [1+i, \; 2+3i, \; 1, \; 1+2i, \; 2i, \; 2, \; 3+i, \; i] \; . \tag{4.6}$$

Then, the $\tilde{x}_r(m)$ defined in (4.1) are obtained as shown in Fig. (4.2). Table (4.1) verifies that

$$[X(3)] = \sum_{r=0}^{5} [G_r(3)] \; . \tag{4.7}$$

---

*A sequence is M-antiperiodic if $x(M+m) = -x(m)$.

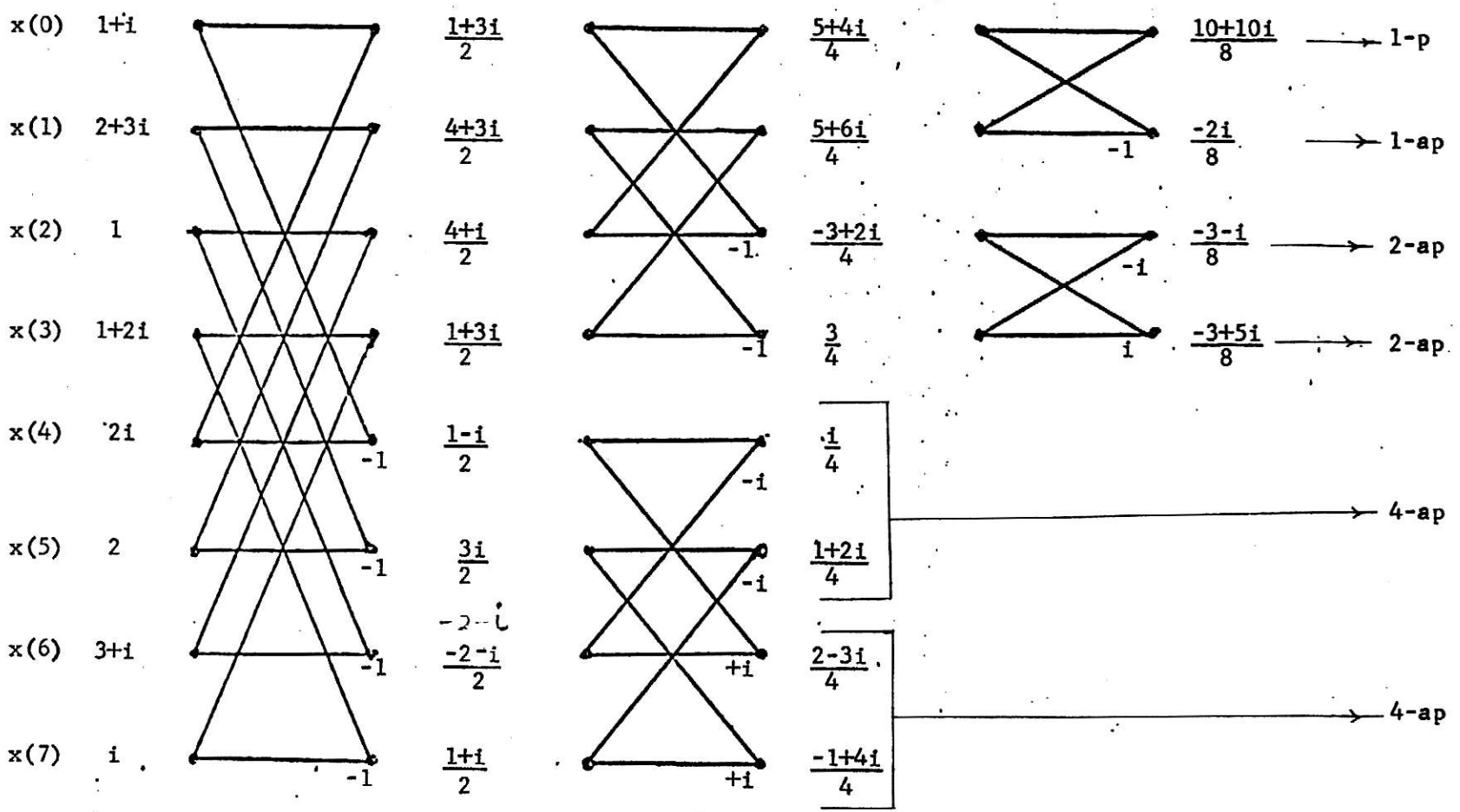

Notation, p = periodic
ap = antiperiodic

Fig. (4.2). Numerical example of decomposition process, N = 8.

Table (4.1)

$[G_0(3)]$	$\frac{10+10i}{8}$	$\frac{10+10i}{8}$	$\frac{10+10i}{8}$	$\frac{10+10i}{8}$	$\frac{10+10i}{8}$	$\frac{10+10i}{8}$	$\frac{10+10i}{8}$	$\frac{10+10i}{8}$	1-p
$[G_1(3)]$	$\frac{-2i}{8}$	$\frac{2i}{8}$	$\frac{-2i}{8}$	$\frac{2i}{8}$	$\frac{-2i}{8}$	$\frac{2i}{8}$	$\frac{-2i}{8}$	$\frac{2i}{8}$	1-ap
$[G_2(3)]$	$\frac{-3-i}{8}$	$\frac{1-3i}{8}$	$\frac{3+i}{8}$	$\frac{-1+3i}{8}$	$\frac{-3-i}{8}$	$\frac{1-3i}{8}$	$\frac{3+i}{8}$	$\frac{-1+3i}{8}$	2-ap
$[G_3(3)]$	$\frac{-3+5i}{8}$	$\frac{5+3i}{8}$	$\frac{3-5i}{8}$	$\frac{-5-3i}{8}$	$\frac{-3+5i}{8}$	$\frac{5+3i}{8}$	$\frac{3-5i}{8}$	$\frac{-5-3i}{8}$	2-ap
$[G_4(3)]$	$\frac{2i}{8}$	$\frac{2+4i}{8}$	$\frac{-2}{8}$	$\frac{-4+2i}{8}$	$\frac{-2i}{8}$	$\frac{-2-4i}{8}$	$\frac{2}{8}$	$\frac{4-2i}{8}$	4-ap
$[G_5(3)]$	$\frac{4-6i}{8}$	$\frac{-2+8i}{8}$	$\frac{-6-4i}{8}$	$\frac{8+2i}{8}$	$\frac{-4+6i}{8}$	$\frac{2-8i}{8}$	$\frac{6+4i}{8}$	$\frac{-8-2i}{8}$	4-ap
$[X(3)]$	1+i	2+3i	1	1+2i	2i	2	3+i	i	8-p

General Structure of $[G_r(n)]$

Inspection of (4.2) reveals that the subsequences $[G_r(3)]$ can be constructed by associating multipliers 1, -1, i and -i with the $\tilde{x}_r(m)$ obtained in Fig. (4.1). A systematic way of associating these multipliers with $\tilde{x}_r(m)$ is shown below.

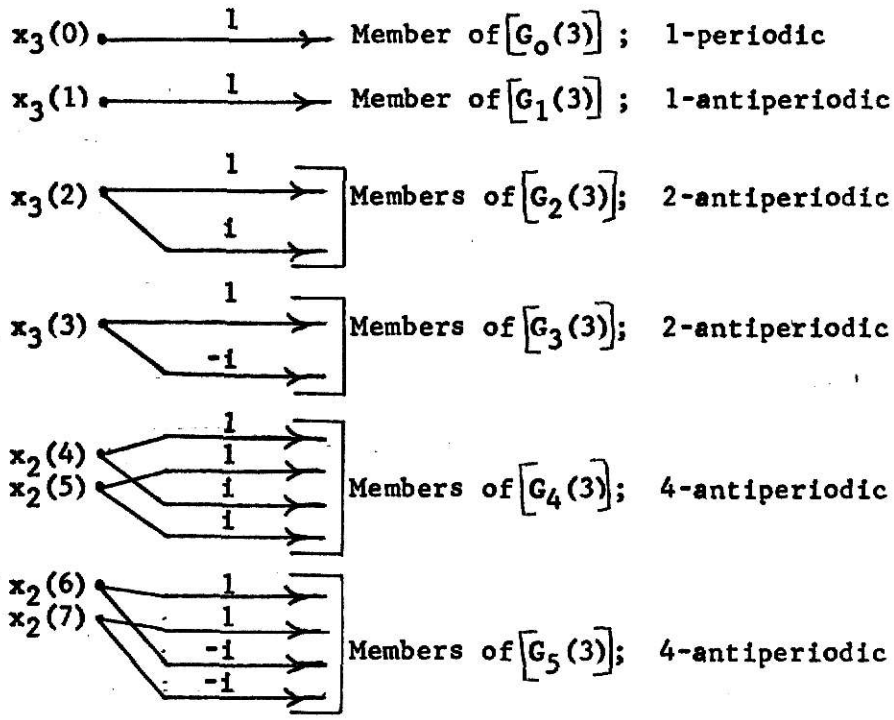

Fig. (4.3). Construction of the subsequences $[G_r(3)]$.

In Fig. (4.3) it is noted that the basic multipliers associated with the 2-antiperiodic sequences are 1, i and 1, -i. The 4-antiperiodic sequences take the same multipliers except that each multiplier appears twice and hence the sets of multipliers are (1, 1, i, i) and (1, 1, -i, -i). Again, if 8-antiperiodic sequences are present then each multiplier appears four times as shown below :

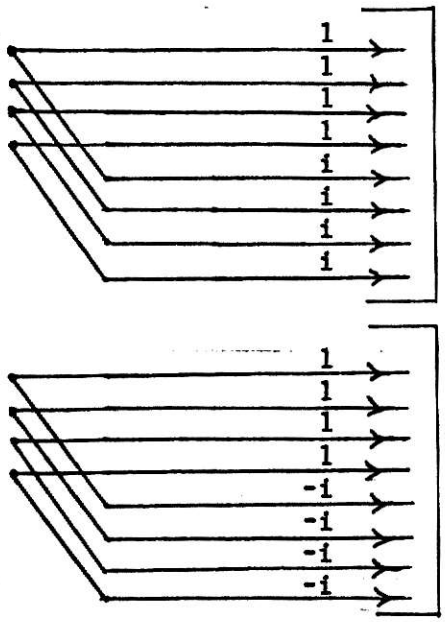

From the above discussion, it follows that in general if m-antiperiodic subsequences $\boxed{G_r(n)}$ are present in the decomposition, then the multipliers 1, i and 1, -i each appears $\frac{m}{2}$ times.

In conclusion, a numerical example for the case N = 16 is considered. Let

$$\boxed{\underline{X}(4)}^T = \boxed{1+i,\ 2+3i,\ \cdots,\ -2i,\ 4} \quad . \tag{4.8}$$

The decomposition process which yields the subsequences $\boxed{G_r(4)}$ is shown in Fig. (4.4). In Table (4.2), it is verified that

$$\boxed{X(4)} = \sum_{r=0}^{7} \boxed{G_r(4)} \quad . \tag{4.9}$$

4.3 Orthogonal Properties of $\boxed{G_r(n)}$

An important property of the subsequences $\boxed{G_r(n)}$ is that they are orthogonal to each other. From the discussion in section 4.1, it is known that a given N-periodic data sequence can be expressed as the sum of 2n subsequences $\boxed{G_r(n)}$. From (4.5) one has

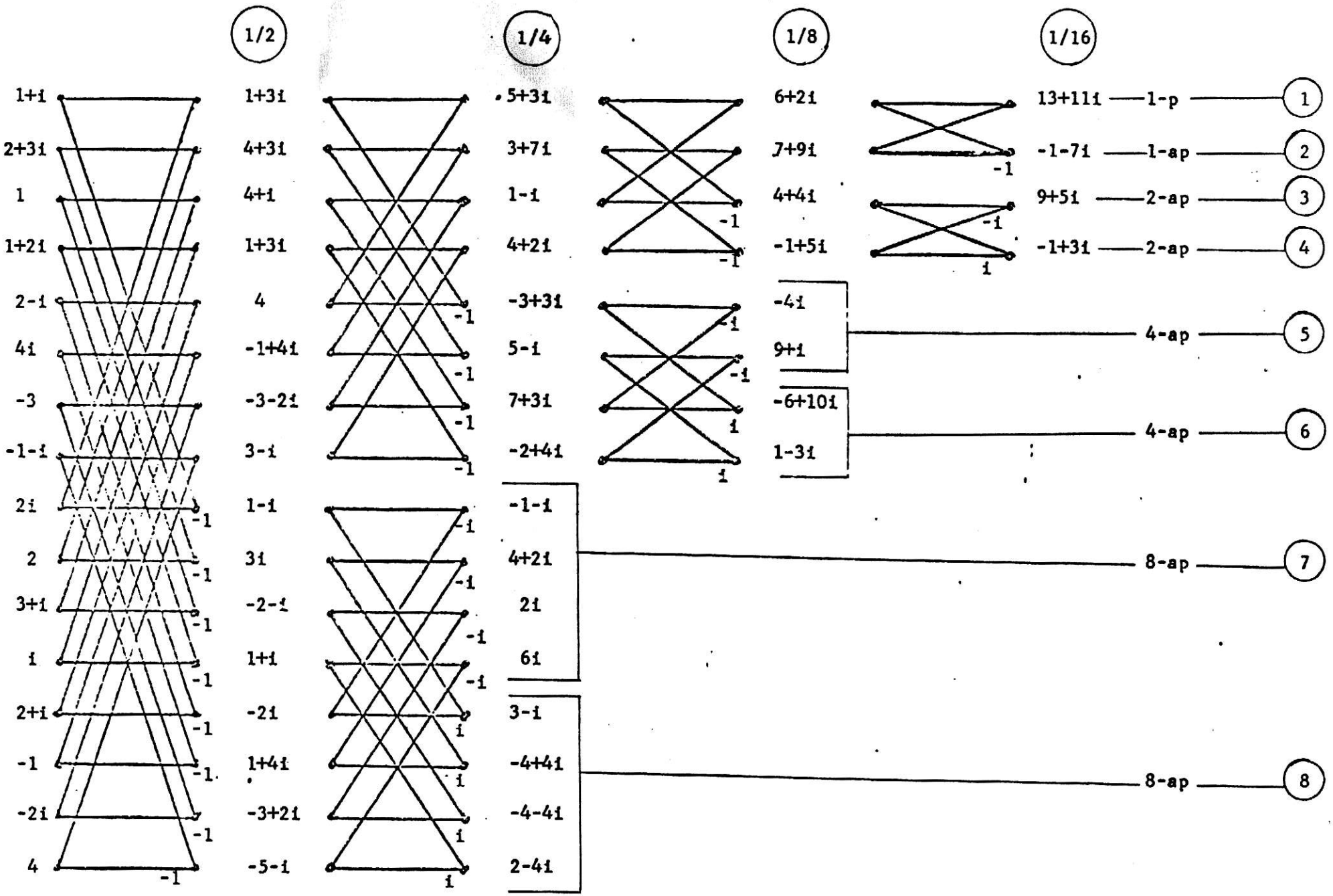

Notation. Number circled above the columns after iteration represents the quantity by which every element in that column should be multiplied.

Table (4,2)

$\frac{13+11i}{16}$	$\frac{13+11i}{16}$	$\frac{13+11i}{16}$	$\frac{13+11i}{16}$	$\frac{13+11i}{16}$	$\frac{13+11i}{16}$	$\frac{13+11i}{16}$	$\frac{13+11i}{16}$
$\frac{-1-7i}{16}$	$\frac{1+7i}{16}$	$\frac{-1-7i}{16}$	$\frac{1+7i}{16}$	$\frac{-1-7i}{16}$	$\frac{1+7i}{16}$	$\frac{-1-7i}{16}$	$\frac{1+7i}{16}$
$\frac{9+5i}{16}$	$\frac{-5+9i}{16}$	$\frac{-9-5i}{16}$	$\frac{5-9i}{16}$	$\frac{9+5i}{16}$	$\frac{-5+9i}{16}$	$\frac{-9-5i}{16}$	$\frac{5-9i}{16}$
$\frac{-1+3i}{16}$	$\frac{3+i}{16}$	$\frac{1-3i}{16}$	$\frac{-3-i}{16}$	$\frac{-1+3i}{16}$	$\frac{3+i}{16}$	$\frac{1-3i}{16}$	$\frac{-3-i}{16}$
$\frac{-8i}{16}$	$\frac{18+2i}{16}$	$\frac{8}{16}$	$\frac{-2+18i}{16}$	$\frac{8i}{16}$	$\frac{-18-2i}{16}$	$\frac{-8}{16}$	$\frac{2-18i}{16}$
$\frac{-12+20i}{16}$	$\frac{2-6i}{16}$	$\frac{20+12i}{16}$	$\frac{-6-2i}{16}$	$\frac{12-20i}{16}$	$\frac{-2+6i}{16}$	$\frac{-20-12i}{16}$	$\frac{6+2i}{16}$
$\frac{-4-4i}{16}$	$\frac{16+8i}{16}$	$\frac{8i}{16}$	$\frac{24i}{16}$	$\frac{4-4i}{16}$	$\frac{-8+16i}{16}$	$\frac{-8}{16}$	$\frac{-24}{16}$
$\frac{12-4i}{16}$	$\frac{-16+16i}{16}$	$\frac{-16-16i}{16}$	$\frac{8-16i}{16}$	$\frac{-4-12i}{16}$	$\frac{16+16i}{16}$	$\frac{-16+16i}{16}$	$\frac{-16-8i}{16}$
$1+i$	$2+3i$	1	$1+2i$	$2-i$	$4i$	-3	$-1-i$

$\frac{13+11i}{16}$	$\frac{13+11i}{16}$	$\frac{13+11i}{16}$	$\frac{13+11i}{16}$	$\frac{13+11i}{16}$	$\frac{13+11i}{16}$	$\frac{13+11i}{16}$	$\frac{13+11i}{16}$
$\frac{-1-7i}{16}$	$\frac{1+7i}{16}$	$\frac{-1-7i}{16}$	$\frac{1+7i}{16}$	$\frac{-1-7i}{16}$	$\frac{1+7i}{16}$	$\frac{-1-7i}{16}$	$\frac{1+7i}{16}$
$\frac{9+5i}{16}$	$\frac{-5+9i}{16}$	$\frac{-9-5i}{16}$	$\frac{5-9i}{16}$	$\frac{9+5i}{16}$	$\frac{-5+9i}{16}$	$\frac{-9-5i}{16}$	$\frac{5-9i}{16}$
$\frac{-1+3i}{16}$	$\frac{3+i}{16}$	$\frac{1-3i}{16}$	$\frac{-3-i}{16}$	$\frac{-1+3i}{16}$	$\frac{3+i}{16}$	$\frac{1-3i}{16}$	$\frac{-3-i}{16}$
$\frac{-8i}{16}$	$\frac{18+2i}{16}$	$\frac{8}{16}$	$\frac{-2+18i}{16}$	$\frac{8i}{16}$	$\frac{-18-2i}{16}$	$\frac{-8}{16}$	$\frac{2-18i}{16}$
$\frac{-12+20i}{16}$	$\frac{2-6i}{16}$	$\frac{20+12i}{16}$	$\frac{-6-2i}{16}$	$\frac{12-20i}{16}$	$\frac{-2+6i}{16}$	$\frac{-20-12i}{16}$	$\frac{6+2i}{16}$
$\frac{4+4i}{16}$	$\frac{-16-8i}{16}$	$\frac{-8i}{16}$	$\frac{-24i}{16}$	$\frac{-4+4i}{16}$	$\frac{8-16i}{16}$	$\frac{8}{16}$	$\frac{24}{16}$
$\frac{-12+4i}{16}$	$\frac{16-16i}{16}$	$\frac{16+16i}{16}$	$\frac{-8+16i}{16}$	$\frac{4+12i}{16}$	$\frac{-16-16i}{16}$	$\frac{16-16i}{16}$	$\frac{16+8i}{16}$
$2i$	2	$3+i$	i	$2+i$	-1	$-2i$	4

$$\left[X(n)\right] = \sum_{r=0}^{2n-1} \left[G_r(n)\right] \; ; \quad n = \log_2 N \; . \tag{4.10}$$

Since each $\left[G_r(n)\right]$ has 2^n elements, it can be expressed as

$$\left[G_r(n)\right] = \left[g_r(0) \quad g_r(1) \quad g_r(2) \quad . \quad . \quad . \quad . \quad g_r(N-1)\right] \; . \tag{4.11}$$

In terms of the elements $g_r(\;)$ of $\left[G_r(n)\right]$, the orthogonal property of the subsequences $\left[G_r(n)\right]$ can be stated as

$$\sum_{m=0}^{N-1} g_r(m) \cdot g_s^{*}(m) = 0 \tag{4.12}$$

for $r \neq s$ and $r, s = 0, 1, 2, \ldots, (2n-1)$., where $g_s^{*}(m)$ is complex conjugate of $g_s(m)$.

4.4 Power Associated with Decomposed Sequence

The purpose of decomposing the given data sequence into 2n subsequences $\left[G_r(n)\right]$, is to establish a one-to-one correspondence between the power in each of these subsequences and a CBT power spectrum point.

It is recalled that the average power in a real M-periodic (or, anti-periodic) sequence

$$\left[X(m)\right] = \left[x(0) \quad x(1) \quad x(2) \cdot \cdot \cdot \cdot x(M-1)\right] \; , \; m = \log_2 M$$

is given by

$$P_{av.} = \frac{1}{M} \sum_{k=0}^{M-1} x^2(k) \; . \tag{4.13}$$

If the M-periodic (or, antiperiodic) sequence is complex, then (4.13) is rewritten in the form

$$P_{av.} = \frac{1}{M} \sum_{k=0}^{M-1} \left| x(k) \right|^2 \tag{4.14}$$

where $\left| x(k) \right|$ denotes the absolute value of x(k).

Consider the 8-periodic sequence defined in (4.6). The powers in corresponding subsequences are computed by applying (4.14) to each of the $\boxed{G_r(3)}$ listed in Table (4.1). Again, the CBT power spectrum for this sequence was computed earlier (see (3.25)). These results are summarized in Table (4.3).

Table (4.3)

Sequence $\boxed{Gr(3)}$	Periodicity	Power Associated	CBT power sepctrum (Ref (3.25))
$\boxed{G_0(3)}$	1-periodic	200/64	P(0) = 200/64
$\boxed{G_1(3)}$	1-antiperiodic	4/64	P(1) = 4/64
$\boxed{G_2(3)}$	2-antiperiodic	10/64	P(2) = 10/64
$\boxed{G_3(3)}$	2-antiperiodic	34/64	P(3) = 34/64
$\boxed{G_4(3)}$	4-antiperiodic	12/64	P(4) = 12/64
$\boxed{G_5(3)}$	4-antiperiodic	60/64	P(5) = 60/64

Similarly results pertaining to the 16-periodic sequence defined in (4.8) obtained from Table (4.2) and (3.26) are summarized in Table (4.4).

Examination of Tables (4.3) and (4.4) reveals that there is a one-to-one correspondence between the CBT power spectrum points P(k) and the subsequences $\boxed{G_r(3)}$ and $\boxed{G_r(4)}$ for N = 8 and N = 16 respectively. In general it can be shown that

1. The CBT power spectrum point P(0) represents the average power in the 1-periodic sequence $\boxed{G_0(n)}$.

2. The CBT power spectrum points P(2s+2) and P(2s+3) respectively represent the average powers in the 2^{s+1}-antiperiodic subsequences $\boxed{G_{2s+2}(n)}$ and $\boxed{G_{2s+3}(n)}$, where $n = \log_2 N$, and $s = 0, 1, 2, \ldots, (n-2)$.

Table (4.4)

Sequence		Power	CBT power spectrum
Gr(4)	Periodicity	Associated	(Refer (3.26))
$G_0(4)$	1-periodic	290/256	P (0) = 290/256
$G_1(4)$	1-antiperiodic	50/256	P (1) = 50/256
$G_2(4)$	2-antiperiodic	106/256	P (2) = 106/256
$G_3(4)$	2-antiperiodic	10/256	P (3) = 10/256
$G_4(4)$	4-antiperiodic	196/256	P (4) = 196/256
$G_5(4)$	4-antiperiodic	292/256	P (5) = 292/256
$G_6(4)$	8-antiperiodic	248/256	P (6) = 248/256
$G_7(4)$	8-antiperiodic	376/256	P (7) = 376/256

CHAPTER V

RECOMMENDATIONS FOR FUTURE WORK

5.1 Relationship Between the CBT and Discrete Fourier Transform (DFT) Spectra

The DFT of a N-periodic sequence is defined as

$$C_x(k) = \sum_{m=0}^{N-1} x(m)\, W^{km}, \quad k = 0, 1, \ldots, (N-1) \qquad (5.1)$$

where $W = e^{-i2\pi/N}$.

The Fast Fourier Transform (FFT) is an algorithm which yields the DFT coefficients $C_x(k)$ in (5.1) in approximately $N \cdot \log_2 N$ arithmetic operations and requires a storage of approximately N locations. The number of storage locations and the number of arithmetic operations required using direct methods to compute the $C_x(k)$ in (5.1) is proportional to N^2. Thus, as N increases, it is obvious that the efficiency of the FFT increases rapidly. As an illustrative example, consider the sequence defined in (4.6), that is

$$\boxed{X(3)} = \boxed{1+i,\ 2+3i, \quad , 3+i,\ i} \ . \qquad (5.2)$$

The FFT signal flow graph, N = 8 is shown in Fig. (5.1). The corresponding power spectrum is obtained as

$$\begin{aligned}
\hat{P}(0) &= \left| C_x(0) \right|^2 = \frac{200}{64} \\
\hat{P}(1) &= \left| C_x(4) \right|^2 = \frac{4}{64} \\
\hat{P}(2) &= \left| C_x(2) \right|^2 = \frac{10}{64} \\
\hat{P}(3) &= \left| C_x(6) \right|^2 = \frac{34}{64} \\
\hat{P}(4) &= \left| C_x(1) \right|^2 = \frac{12+2\sqrt{2}}{64} \\
\hat{P}(5) &= \left| C_x(5) \right|^2 = \frac{12-2\sqrt{2}}{64} \\
\hat{P}(6) &= \left| C_x(3) \right|^2 = \frac{60+38\sqrt{2}}{64} \\
\hat{P}(7) &= \left| C_x(7) \right|^2 = \frac{60-38\sqrt{2}}{64} \ .
\end{aligned} \qquad (5.3)$$

$$A_2 = -1,\ A_4 = -i,\ A_8 = \frac{1-i}{2}$$

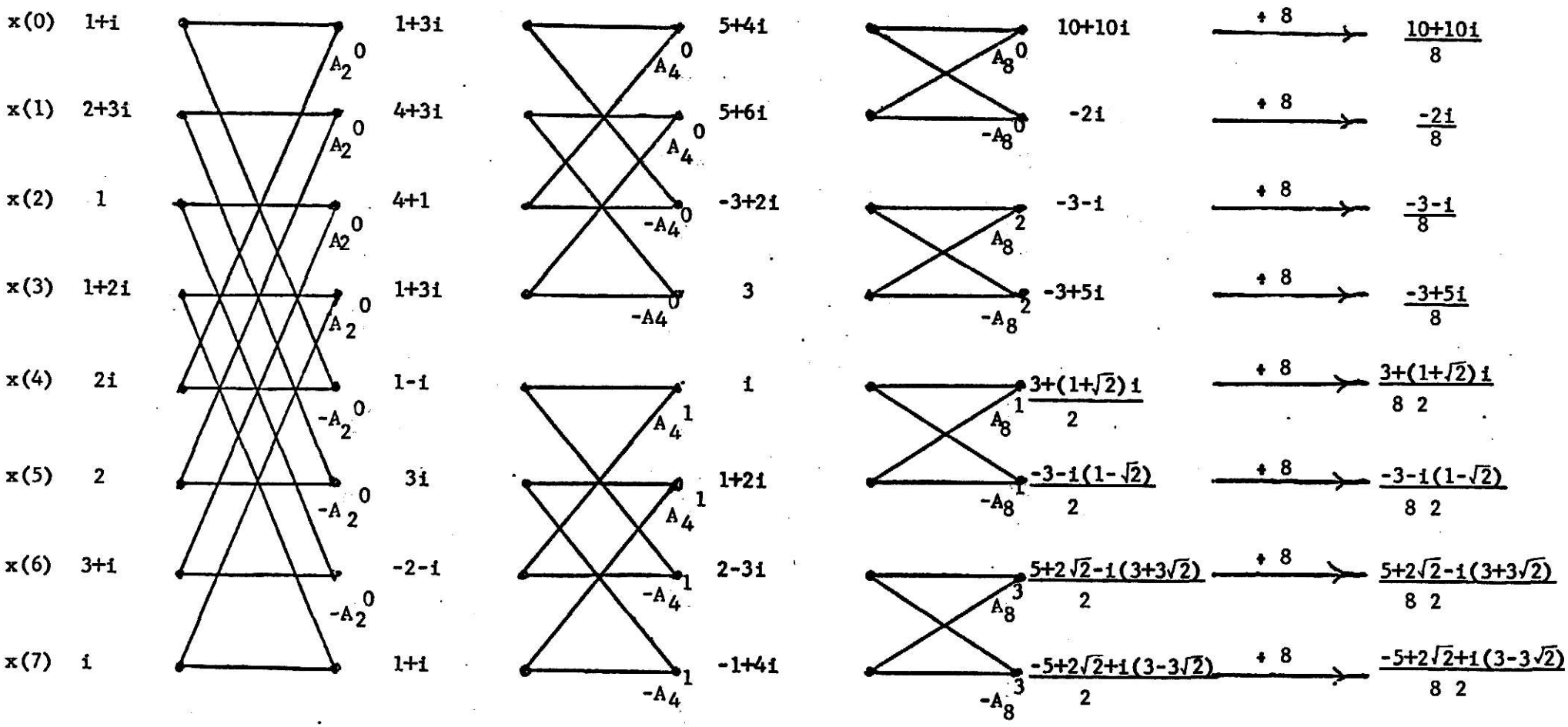

Fig. (5.1). FFT signal flow graph for N = 8.

Comparing this flow graph with the CBT signal flow graph for N = 8, it is apparent that the two are very similar. On the basis of this similarity, the following recommendations are made for future work:

1. Develop a general transformation which relates the discrete Fourier and complex BIFORE transform.

2. Determine the relation between the CBT and DFT power spectra. The DFT power spectrum is defined as

$$\hat{P}(s) = \left|C_x(s)\right|^2, \; s = 0, 1, \ldots, (N-1) . \tag{5.4}$$

For the simple example of the 8-periodic sequence in (5.2), it is straightforward to verify that

$$\begin{aligned} P(s) &= \hat{P}(s), \; s = 0, 1, 2, 3 \\ P(4) &= \hat{P}(4) + \hat{P}(5) \\ \text{and} \quad P(5) &= \hat{P}(6) + \hat{P}(7) \end{aligned} \tag{5.5}$$

where, the P(s) are the CBT power spectrum points (see (3.25)). This suggests the existence of a general rule to obtain P(s), given $\hat{P}(s)$.

3. When the data sequence $\boxed{\underline{X}(n)}$ is real, then it is known that $(\frac{N}{2} + 1)$ of the $\hat{P}(s)$ and $(\log_2 N + 1)$ of P(s) are independent spectrum points. Again, when $\boxed{\underline{X}(n)}$ is complex, the DFT and CBT yield N and $2\log_2 N$ independent spectrum points. It is emphasized that both spectra represent a distribution of power in $\boxed{\underline{X}(n)}$ and have the shift invariant property. Thus it is instructive to investigate whether there are other transforms and corresponding power spectra, whose number of spectrum points falls between the limits cited above.

SELECTED REFERENCES

1. W. T. Cochran, J. W. Cooley, et. al., "The Fast Fourier Transform," Proc. IEEE. October 1967, pp. 1664-1674.

2. J. E. Whelchel and D. F. Guinn, "The Fast Fourier-Hadamard Transform and Its Use in Signal Representation and Classification," EASCON '68. Record, pp. 561-573.

3. F. R. Ohnsorg, "Binary Fourier Representation," Spectrum Analysis Techniques Symposium, Sept. 1966, Honeywell Research Center, Hopkins, Minnesota.

4. S. W. Golomb, et. al., Digital Communications, Prentice-Hall, Inc., 1964, pp. 53-62.

5. W. K. Pratt, et. al., "Hadamard Transform Image Coding," Proc. IEEE, vol. 57, pp. 58-68, January 1968.

6. N. Ahmed and K. R. Rao, "Spectral Analysis of Linear Time-Invariant Systems Using BIFORE (Binary Fourier Representation)," Electronics Letters, vol. 6, No. 2, 22nd. Jan., 1970, pp. 43-44.

7. W. R. Crowther and C. M. Rader, "Efficient Coding of Vocoder Channel Signals Using Linear Transformation," Proc. IEEE, 65, pp. 1594-1595, November 1966.

8. S. J. Campanella and G. S. Robinson, "Digital Sequency Decomposition of Voice Signals," Proc. of the Walsh Function Symposium, Naval Research Laboratory, Washington, D.C., March 31 - April 3, 1970, pp. 230-237.

9. N. Ahmed and K. R. Rao, "Discrete Fourier and Hadamard Transforms," Electronics Letters, Vol. 6, 2nd April 1970, pp. 221-224.

10. N. Ahmed and K. R. Rao, "Convolution and Correlation Using Binary Fourier Representation," Proceedings of the First Annual Houston Conference on Circuits, Systems, and Computers, May 22-23, 1969, Houston, Texas.

11. F. R. Ohnsorg, "Application of Walsh Functions to Complex Signals," Office of Central Theory and Applications, NASA Electronics and Research Center, Cambridge, Mass., Proc. of the Walsh Function Symposium, Naval Research Laboratory, Washington, D.C., March 31 - April 3, 1970, pp. 123-127.

12. C. C. Macdauffee, An Introduction to Abstract Algebra, John Wiley and Sons, 1940.

APPENDIX A

Kronecker delta matrix product (denoted by $\otimes$) is explained below considering two square matrices

$$\begin{bmatrix} a & b \\ c & d \end{bmatrix} \otimes \begin{bmatrix} e & f & g \\ h & i & j \\ k & l & m \end{bmatrix} = \begin{bmatrix} a\begin{bmatrix} e & f & g \\ h & i & j \\ k & l & m \end{bmatrix} & b\begin{bmatrix} e & f & g \\ h & i & j \\ k & l & m \end{bmatrix} \\ c\begin{bmatrix} e & f & g \\ h & i & j \\ k & l & m \end{bmatrix} & d\begin{bmatrix} e & f & g \\ h & i & j \\ k & l & m \end{bmatrix} \end{bmatrix}$$

$$= \begin{bmatrix} ae & af & ag & be & bf & bg \\ ah & ai & aj & bh & bi & bj \\ ak & al & am & bk & bl & bm \\ ce & cf & cg & de & df & dg \\ ch & ci & cj & dh & di & dj \\ ck & cl & cm & dk & dl & dm \end{bmatrix} .$$

In general, if a matrix A of order (mxm) and a matrix B of order (nxn) are multiplied in Kronecker delta manner, then the resulting matrix is of order (mn x mn).

It is recalled that $[H_c(2)]$ can be written as

$$[H_c(2)] = \left[\begin{array}{cc|cc} 1 & 1 & 1 & 1 \\ 1 & -1 & 1 & -1 \\ \hline 1 & -i & -1 & i \\ 1 & i & -1 & -i \end{array}\right] .$$

A matrix $[P(1)]$ of order (2 x 2) is defined as

$$\left[P(1)\right] = \begin{bmatrix} 1 & -i \\ 1 & i \end{bmatrix} .$$

Then $\left[H_c(2)\right]$ can be written as

$$\left[H_c(2)\right] = \left[\begin{array}{c|c} \dfrac{H_c(1)}{P(1) \otimes H(0)} & \dfrac{H_c(1)}{-P(1) \otimes H(0)} \end{array}\right]$$

where $\left[H(0)\right] = \left[1\right]$. The above result is generalized to obtain

$$\left[H_c(n)\right] = \left[\begin{array}{c|c} \dfrac{H_c(n-1)}{P(1) \otimes H(n-2)} & \dfrac{H_c(n-1)}{-P(1) \otimes H(n-2)} \end{array}\right] . \qquad \text{(A.1)}$$

It can be simplified by using

$$\left[P(1)\right] \otimes \left[H(n-2)\right] = \begin{bmatrix} 1 & -i \\ 1 & i \end{bmatrix} \left[H(n-2)\right]$$

$$= \left[\begin{array}{c|c} H(n-2) & -iH(n-2) \\ \hline H(n-2) & iH(n-2) \end{array}\right]$$

which leads (A.1) to yield

$$\left[H_c(n)\right] = \left[\begin{array}{c|c|c|c} H_c(n-1) & & H_c(n-1) & \\ \hline H(n-2) & -iH(n-2) & -H(n-2) & iH(n-2) \\ \hline H(n-2) & iH(n-2) & -H(n-2) & -iH(n-2) \end{array}\right] . \qquad \text{(A.2)}$$

Using (A.2) $\left[H_c(3)\right]$ can be derived from $\left[H_c(2)\right]$ as follows

$$\left[H_c(3)\right] = \left[\begin{array}{c|c|c|c} H_c(2) & & H_c(2) & \\ \hline H(1) & -iH(1) & -H(1) & iH(1) \\ \hline H(1) & iH(1) & -H(1) & -iH(1) \end{array}\right]$$

$$
= \left[\begin{array}{cccc|cccc}
1 & 1 & 1 & 1 & 1 & 1 & 1 & 1 \\
1 & -1 & 1 & -1 & 1 & -1 & 1 & -1 \\
\hline
1 & -i & -1 & i & 1 & -i & -1 & i \\
1 & i & -1 & -i & 1 & i & -1 & -i \\
\hline
1 & 1 & -i & -i & -1 & -1 & i & i \\
1 & -1 & -i & i & -1 & 1 & i & -i \\
1 & 1 & i & i & -1 & -1 & -i & -i \\
1 & -1 & i & -i & -1 & 1 & -i & i
\end{array}\right] .
$$

Higher order $\left[H_c\right]$ can be computed in a similar manner.

APPENDIX B

In (3.6) the shift matrix $[A(3)]$ was calculated. It has the block diagonal structure as shown below :

$$[A(3)] = \text{diagonal } [A_0, A_1, A_2, A_3, A_4, A_5]$$

where

$$[A_0] = [1]$$

$$[A_1] = [-1]$$

$$[A_2] = [i]$$

$$[A_3] = [-i]$$

$$[A_4] = \begin{bmatrix} \frac{1+i}{2} & \frac{-1+i}{2} \\ \frac{1-i}{2} & \frac{-1-i}{2} \end{bmatrix}$$

and

$$[A_5] = \begin{bmatrix} \frac{1-i}{2} & \frac{-1-i}{2} \\ \frac{1+i}{2} & \frac{-1+i}{2} \end{bmatrix} . \qquad \text{(B.1)}$$

It should be noted that

$$[A_3] = [A_2^*]$$

and

$$[A_5] = [A_4^*] . \qquad \text{(B.2)}$$

For shift matrix in real BT a recursive relationship is derived which is based on the roots of the characteristic equation [11] .

Factorization of the characteristic polynomial

$$A^N - 1 = 0 \qquad \text{(B.3)}$$

over the real field generates the following shift matrix

$$[A(n)] = \text{diagonal } [A_0, A_1, A_2, A_3, A_4, \ldots\ldots, A_{N-1}] \qquad \text{(B.4)}$$

The characteristic equation given in (B.3) when factorized over the complex field yields

$$A^N - 1 = (A-1) \prod_{k=0}^{n-1} \left[(A)^{2^k} + 1 \right] \qquad (B.5)$$

which governs the shift matrix in this case [12] . The shift matrix is of block diagonal structure and can be defined as

$$[A(n)] = \text{diagonal} \left[A_1(0) \quad A_2(0) \quad C_1(0) \quad C_2(0) \quad C_1(1) \quad C_2(1) \; . \; . \; . \; . \; . \; . \; C_1(n-2) \quad C_2(n-2) \right] \qquad (B.6)$$

where

$$[A_1(0)] = [1]$$
$$[A_2(0)] = [-1]$$

and $[C_1(k)]$ and $[C_2(k)]$ are square matrices of order 2^k and complex conjugate of each other.

A recursive relationship to compute $[C_1(k)]$ and $[C_2(k)]$ is derived below [11].

Considering N = 4, a sequence shifted by one position to left can be related to the original data sequence $[X(2)]$ as

$$[\underline{X}^{(1)}(2)] = [M(2)] \; [\underline{X}(2)] \qquad (B.7)$$

where the transformation matrix $[M(2)]$ is

$$[M(2)] = \begin{bmatrix} 0 & 1 & 0 & 0 \\ 0 & 0 & 1 & 0 \\ 0 & 0 & 0 & 1 \\ 1 & 0 & 0 & 0 \end{bmatrix} .$$

Now, a matrix $[U(n)]$ of order $(2^n \times 2^n)$ is defined which has all zero elements except the element in the first column and last row, which is 1.

Using $[U(n)]$ a recursive relationship for $[M(n)]$ can be written as

$$[M(n+1)] = \left[\begin{array}{c|c} M(n) - U(n) & U(n) \\ \hline U(n) & M(n) - U(n) \end{array}\right] . \qquad (B.8)$$

For n = 1, $[M(2)]$ can be written as

$$[M(2)] = \left[\begin{array}{cc|cc} 0 & 1 & 0 & 0 \\ 1 & 0 & 1 & 0 \\ \hline 0 & 0 & 0 & 1 \\ 1 & 0 & 1 & 0 \end{array}\right] - \left[\begin{array}{cc|cc} 0 & 0 & 0 & 0 \\ 1 & 0 & 1 & 0 \\ \hline 0 & 0 & 0 & 0 \\ 1 & 0 & 1 & 0 \end{array}\right]$$

or

$$[M(2)] = \begin{bmatrix} 0 & 1 & 0 & 0 \\ 0 & 0 & 1 & 0 \\ 0 & 0 & 0 & 1 \\ 1 & 0 & 0 & 0 \end{bmatrix} .$$

The recursive formula for $[C_m(k)]$ is

$$[C_m(k)] = [H(k)]^{-1} \left[[M(k)] - [U(k)] + (-1)^{m+1} i [U(k)] \right] [H(k)] \qquad (B.9)$$

where m = 1, 2 and $[H(k)]$ is $(2^k)^{th}$ order Hadamard matrix $[11]$.

Using (B.9), $[C_1(1)]$ is computed to be

$$[C_1(1)] = [H(1)]^{-1} \left[[M(1)] - [U(1)] + (-1)^2 i [U(1)] \right] [H(1)]$$

or

$$[C_1(1)] = \frac{1}{2} \begin{bmatrix} 1 & 1 \\ 1 & -1 \end{bmatrix} \left(\begin{bmatrix} 0 & 1 \\ 1 & 0 \end{bmatrix} - \begin{bmatrix} 0 & 0 \\ 1 & 0 \end{bmatrix} + i \begin{bmatrix} 0 & 0 \\ 1 & 0 \end{bmatrix} \right) \begin{bmatrix} 1 & 1 \\ 1 & -1 \end{bmatrix}$$

$$\text{or} \quad \left[C_1(1)\right] = \frac{1}{2}\begin{bmatrix} 1+i & -1+i \\ 1-i & -1-i \end{bmatrix}$$

$$\text{and} \quad \left[C_2(1)\right] = \left[C_1^*(1)\right] = \frac{1}{2}\begin{bmatrix} 1-i & -1-i \\ 1+i & -1+i \end{bmatrix}$$

which was calculated in (3.8).

To illustrate the recursion, $\left[C_1(2)\right]$ is computed. From (B.9)

$$\left[C_1(2)\right] = \left[H(2)\right]^{-1}\left[\left[M(2)\right] - \left[U(2)\right] + (-1)^2 i\left[U(2)\right]\right]\left[H(2)\right]$$

$$\text{or} \quad \left[C_1(2)\right] = \frac{1}{4}\begin{bmatrix} 1 & 1 & 1 & 1 \\ 1 & -1 & 1 & -1 \\ 1 & 1 & -1 & -1 \\ 1 & -1 & -1 & 1 \end{bmatrix}\left[\begin{bmatrix} 0 & 1 & 0 & 0 \\ 0 & 0 & 1 & 0 \\ 0 & 0 & 0 & 1 \\ 1 & 0 & 0 & 0 \end{bmatrix} - \begin{bmatrix} 0 & 0 & 0 & 0 \\ 0 & 0 & 0 & 0 \\ 0 & 0 & 0 & 0 \\ 1 & 0 & 0 & 0 \end{bmatrix} + i\begin{bmatrix} 0 & 0 & 0 & 0 \\ 0 & 0 & 0 & 0 \\ 0 & 0 & 0 & 0 \\ 1 & 0 & 0 & 0 \end{bmatrix}\right]\begin{bmatrix} 1 & 1 & 1 & 1 \\ 1 & -1 & 1 & -1 \\ 1 & 1 & -1 & -1 \\ 1 & -1 & -1 & 1 \end{bmatrix}$$

$$\text{or} \quad \left[C_1(2)\right] = \frac{1}{4}\begin{bmatrix} 3+i & -1+i & -1+i & -1+i \\ 1-i & -3-i & 1-i & 1-i \\ 1-i & 1-i & 1-i & -3-i \\ -1+i & -1+i & 3+i & -1+i \end{bmatrix}$$

$$\text{and} \quad \left[C_2(2)\right] = \left[C_1^*(2)\right]$$

Higher order block diagonal matrices can be computed in a similar way using (B.9).

ACKNOWLEDGEMENT

The author wishes to express his sincere thanks to his major professor, Dr. Nasir Ahmed, for his ready and invaluable assistance and encouragement during the course of this work.

THE COMPLEX BINARY FOURIER REPRESENTATION

by

TEJKARAN R. AGRAWAL

B. E. (Elect. Engg.), 1968
Shri G. S. Technological Institute,
University of Indore, Indore (M. P.)
INDIA

AN ABSTRACT OF A MASTER'S REPORT

submitted in partial fulfillment of the

requirements for the degree

MASTER OF SCIENCE

Department of Electrical Engineering

KANSAS STATE UNIVERSITY
Manhattan, Kansas

1970

ABSTRACT

The Complex BIFORE (Binary Fourier Representation) transform (CBT) is studied. An algorithm which yields the inverse CBT in approximately $N\log_2 N$ arithmetic operations is developed.

The CBT power spectrum is compared with corresponding power spectrum of the BIFORE transform (BT) and discrete Fourier transform. An algorithm which enables rapid computation of the CBT power spectrum is developed. Again, a physical interpretation of the CBT power spectrum is provided. This is accomplished by developing a method which enables a real or complex N-periodic data sequence to be expressed as the sum of $2\log_2 N$ mutually orthogonal subsequences.